Supporting information

Influence of Hydroxycoumarin Substituents on the Photophysical properties of Chiroptical Tb(III) and Eu(III) Complexes

Silvia Ruggieri,[1] Silvia Mizzoni,[1] Enrico Cavalli,[2] Cristina Sissa,[2] Michele Anselmi,[3] Andrea Gualandi,[3,4] Pier Giorgio Cozzi,[3,4] Albano N. Carneiro Neto,[5] Andrea Melchior,[6*] Francesco Zinna,[7] Oliver G. Willis,[7] Lorenzo Di Bari,[7*] Fabio Piccinelli[1*]

[1] Luminescent Materials Laboratory, DB, University of Verona, and INSTM, UdR Verona, Strada Le Grazie 15, 37134 Verona, Italy
[2] Department of Chemistry, Life Sciences and Environmental Sustainability, University of Parma Parco Area delle Scienze, 17/a – 43124, Parma, Italy
[3] Department of Chemistry "G. Ciamician", University of Bologna, via Gobetti 85 – 40129, Bologna, Italy
[4] Center for Chemical Catalysis - C3, University of Bologna, via Gobetti 85, 40129, Bologna, Italy
[5] Physics Department and CICECO – Aveiro Institute of Materials, University of Aveiro, 3810-193, Aveiro, Portugal
[6] Polytechnic Department of Engineering, Laboratory of Chemical Technologies, University of Udine, via Cotonificio 108, 33100 Udine, Italy
[7] Department of Chemistry and Industrial Chemistry, University of Pisa, via Moruzzi 13, 56124 Pisa, Italy

*corresponding authors' email address: fabio.piccinelli@univr.it, lorenzo.dibari@unipi.it and andrea.melchior@uniud.it

Contents

Supporting information

1. General methods and materials

^{1}H-NMR spectra were recorded on Varian Mercury 400 spectrometer or Bruker 600 spectrometer. Chemical shifts are reported in ppm from TMS with the solvent resonance as the internal standard ($CDCl_3$: δ = 7.24 ppm). Data are reported as follows: chemical shift, multiplicity (s = singlet, d = doublet, t = triplet, q = quartet, m= multiplet, bs = broad singlet), coupling constants (Hz), number of protons. ^{13}C-NMR spectra were recorded on Varian Mercury 400 spectrometer or Bruker 600 spectrometer. Chemical shifts are reported in ppm from TMS with the solvent as the internal standard ($CDCl_3$: δ = 77.0 ppm). HPLC-MS analyses were performed on an Agilent Technologies HP1100 instrument coupled with an Agilent Technologies MSD1100 single-quadrupole mass spectrometer using a Phenomenex Gemini C18 3 µm (100 x 3 mm) column; mass spectrometric detection was performed in full-scan mode from *m/z* 50 to 2500, scan time 0.1 s in positive ion mode, ESI spray voltage 4500 V, nitrogen gas 35 psi, drying gas flow rate 11.5 mL·min^{-1}, fragmentor voltage 30 V. Mass are reported as *m/z*, relative intensity, ion. Chromatographic purifications were done with 240-400 mesh silica gel. All reactions were set up under an argon atmosphere in oven-dried glassware using standard Schlenk techniques. All the reagents were purchased from commercial sources (Sigma-Aldrich, Alfa Aesar, Fluorochem, Strem Chemicals, TCI) and used without further purification unless specified. Anhydrous solvents were supplied by Aldrich in Sureseal® bottles and, unless specified, were used without further treatment.

1.1. Synthesis of ***Coum A*** *and* ***Coum D***

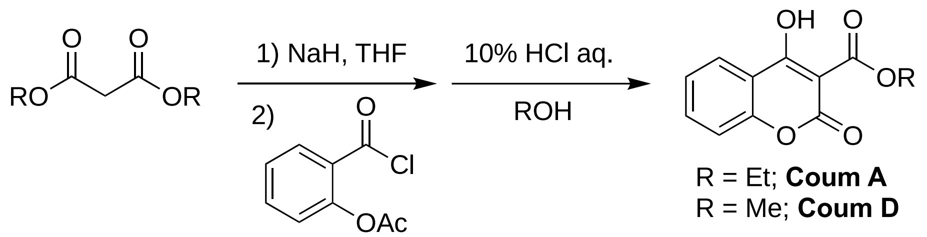

The compounds were prepared by modified literature procedure.[1] A suspension of NaH (60% in mineral oil, 9.09 mmol, 363 mg, 1.8 equiv.) in anhydrous THF (6 mL) was stirred at 0°C for 15 minutes. A solution of malonate (7.58 mmol, 1.5 equiv.) in THF (4 mL) was added dropwise at 0°C and the mixture was stirred for 10 minutes at the same temperature and 1 hour at room temperature. A solution of *O*-acetylsalicyloyl chloride (5.05 mmol, 1g) in THF (4 mL) was added dropwise at 0°C and the mixture was stirred for 10 minutes at the same temperature and 2 hours at room temperature.

Supporting information

The solvent was evaporated and the residue was acidified with 10% HCl (15 mL) at 0°C and extracted with DCM (3 × 20 mL). The combined organic layers were dried over Na_2SO_4 and the solvent evaporated under reduced pressure. The residue was dissolved in 10 mL of ethanol (for **Coum A**) or methanol (for **Coum D**) and 10% HCl (10 mL) was added. The mixture was stirred for 48 hours and the solvent was evaporated. Water (10 mL) was added to the residue and extraction with DCM (3 × 20 mL) was performed. The combined organic layers were dried over Na_2SO_4 and the solvent evaporated under reduced pressure. The product was purified by flash chromatography (SiO_2, from 65:35:1 to 75:25:1 DCM:cyclohexane:AcOH) to give white solids in stated yields.

Spectroscopic data are in agreement with those reported in the literature.[1,2]

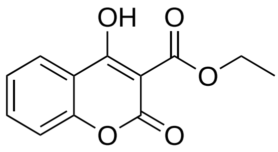

Coum A: 64% yield (3.2 mmol, 756 mg); white solid; m.p. = 97 – 98 °C (lit. m.p. = 97 – 98 °C) [3]; ^{1}H NMR (600 MHz, $CDCl_3$) δ 14.71 (s, 1H), 7.98 (ddd, J = 8.0, 1.7, 0.5 Hz, 1H), 7.64 (ddd, J = 8.4, 7.3, 1.7 Hz, 1H), 7.32–7.25 (m, 2H), 4.48 (q, J = 7.1 Hz, 2H), 1.43 (t, J = 7.1 Hz, 3H), ^{13}C NMR (151 MHz, $CDCl_3$) δ 175.4, 171.9, 157.3, 154.4, 135.5, 125.0, 124.2, 116.8, 114.4, 93.1, 62.8, 14.1; MS (ESI+) *m/z* = 235.0 (81, $[M+H]^+$), 257.0 (85, $[M+Na]^+$), 363.0 (33, $[3M+Na+H]^{2+}$), 371.0 (100, $[3M+K+H]^{2+}$), 490.9 (91, $[2M+Na]^+$).

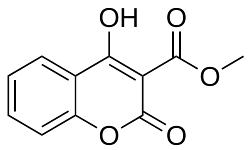

Coum D: 52% yield (2.6 mmol, 576 mg); white solid; m.p. = 138 – 139 °C (lit. m.p. = 137 – 138 °C) [3]; ^{1}H NMR (600 MHz, $CDCl_3$) δ 14.58 (bs, 1H), 8.00 (ddd, J = 8.0, 1.7, 0.6 Hz, 1H), 7.66 (ddd, J = 8.4, 7.3, 1.6 Hz, 1H), 7.35 – 7.26 (m, 2H), 4.02 (s, 3H); ^{13}C NMR (151 MHz, $CDCl_3$) δ 175.5, 172.3, 157.5, 154.4, 135.7, 125.1, 124.3, 116.9, 114.4, 92.9, 53.3; MS (ESI+) *m/z* = 221.0 (72, $[M+H]^+$), 243.0 (64, $[M+Na]^+$), 342.0 (35, $[3M+Na+H]^{2+}$), 350.0 (100, $[3M+K+H]^{2+}$), 462.9 (88, $[2M+Na]^+$).

Supporting information

1.2. Synthesis of ***Coum B***

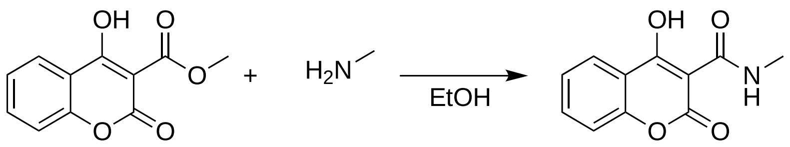

To a solution of **Coum D** (0.68 mmol, 150 mg) in ethanol under nitrogen atmosphere a solution of methylamine (33% wt. in ethanol, 24 mmol, 3 ml) was added. The reaction was stirred at room temperature until complete consumption of the starting material (verified by ^{1}H NMR analysis). The solvent was removed under reduced pressure and the product was purified by flash chromatography (SiO_2, 90:10 DCM:cyclohexane) to give a white solid in 65% yield (0.41 mmol, 90 mg).

Spectroscopic data are in agreement with those reported in the literature.[3]

m.p. = 184 – 185 °C (lit. m.p.: 200 – 202 °C)[4]; ^{1}H NMR (600 MHz, $CDCl_3$) δ 9.15 (bs, 1H), 8.02 (ddd, J = 8.0, 1.7, 0.5 Hz, 1H), 7.64 (ddd, J = 8.3, 7.3, 1.7 Hz, 1H), 7.36 – 7.27 (m, 2H), 3.01 (d, J = 5.0 Hz, 3H), ^{13}C NMR (151 MHz, CDCl3) δ 176.8, 171.1, 162.7, 153.4, 134.8, 125.1, 124.5, 116.9, 116.1, 91.6, 25.99; MS (ESI+) *m/z* = 220.1 (100, $[M+H]^+$), 241.9 (44, $[M+Na]^+$), 339.9 (43, $[3M+Na+H]^{2+}$), 347.9 (41, $[3M+K+H]^{2+}$), 460.9 (16, $[2M+Na]^+$); 476.9 (19, $[2M+K]^+$).

1.3. Synthesis of ***Coum C***

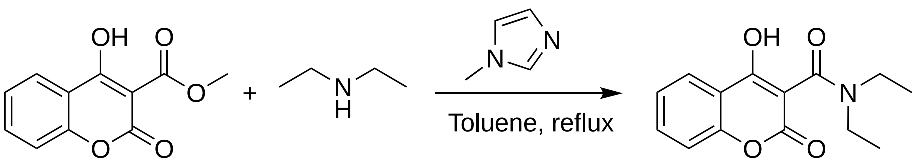

To a solution of **Coum D** (0.45 mmol, 100 mg) in anhydrous toluene (3 mL) under nitrogen atmosphere, diethylammine (1.8 mmol, 186 µL, 4 equiv.) and N-methylimidazole (0.55 mmol, 44 µL, 1.2 equiv.) were added. The mixture was refluxed for 24 hours and the solvent was removed under reduced pressure. The residue was dissolved in $CHCl_3$ (20 mL) and washed with 1M HCl aq. (2 x 10 mL), the combined organic layers were dried over Na_2SO_4 and the solvent evaporated under reduced pressure. The product was purified by flash chromatography (SiO_2, from 100% AcOEt to 90:10 AcOEt:MeOH) to give a white solid in 73% yield (0.41 mmol, 105 mg).

Supporting information

m.p. = 184 – 185 °C; ^{1}H NMR (401 MHz, $CDCl_3$) δ 12.09 (bs, 1H), 7.89 (dd, J = 8.0, 1.7 Hz, 1H), 7.60 – 7.46 (m, 1H), 7.30 – 7.14 (m, 2H), 3.44 (q, J = 7.1 Hz, 4H), 1.23 (t, J = 7.1 Hz, 6H), ^{13}C NMR (101 MHz, $CDCl_3$) δ 171.8, 171.7, 168.4, 159.1, 153.6, 133.9, 124.5, 124.0, 116.4, 115.4, 96.8, 42.2, 12.9; MS (ESI+) *m/z* = 262.1 (100, $[M+H]^+$), 283.9 (40, $[M+Na]^+$), 402.9 (34, $[3M+Na+H]^{2+}$), 410.9 (40, $[3M+K+H]^{2+}$), 544.9 (18, $[2M+Na]^+$); 560.9 (10, $[2M+K]^+$).

1.4. NMR characterization of the coumarins

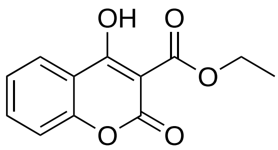

^{1}H NMR (600 MHz, $CDCl_3$)

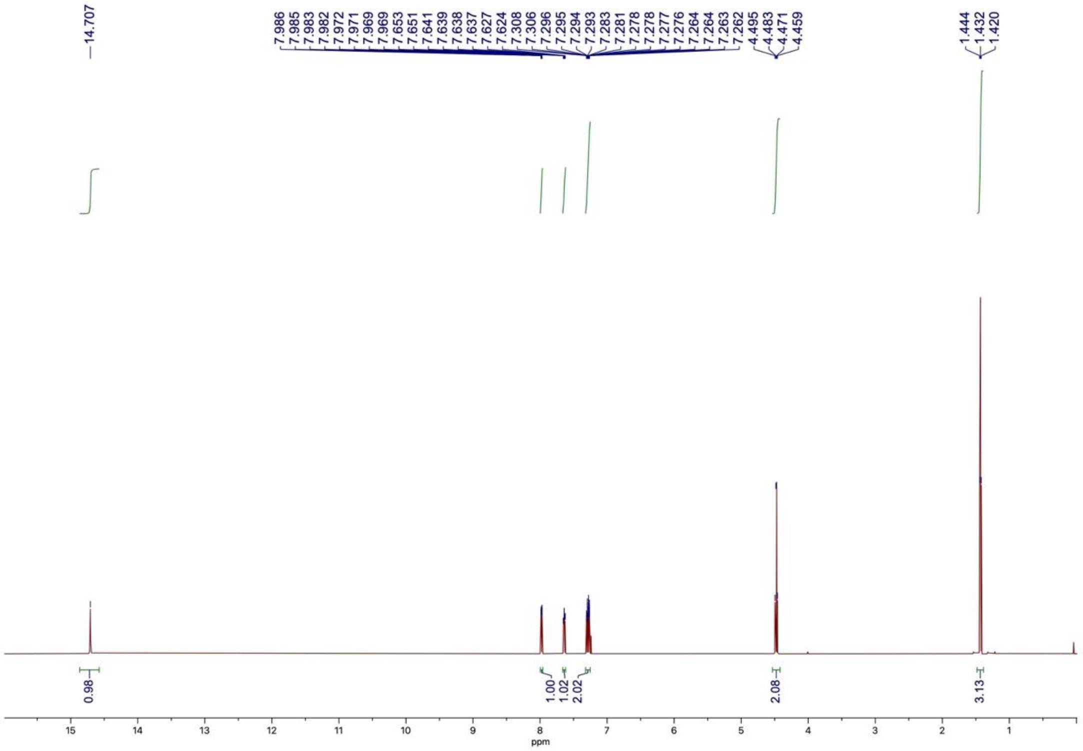

{1H}^{13}C NMR (151 MHz, $CDCl_3$)

Supporting information

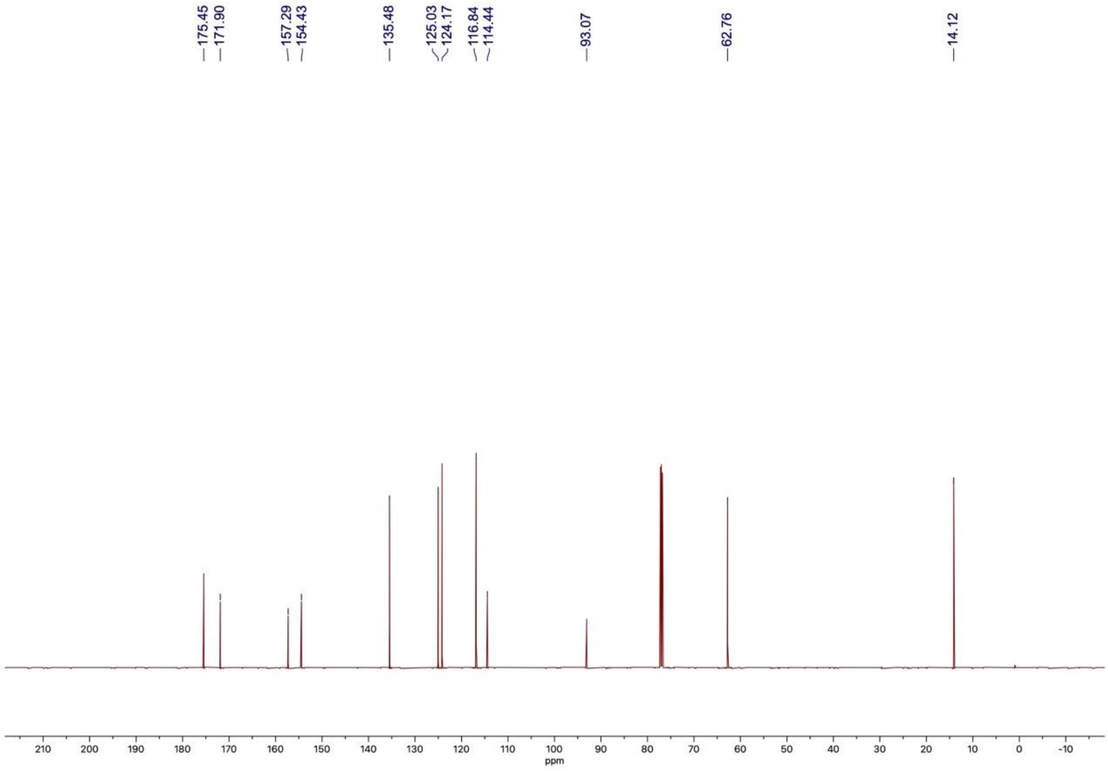

Supporting information

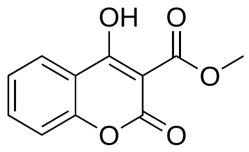

^{1}H NMR (600 MHz, $CDCl_3$)

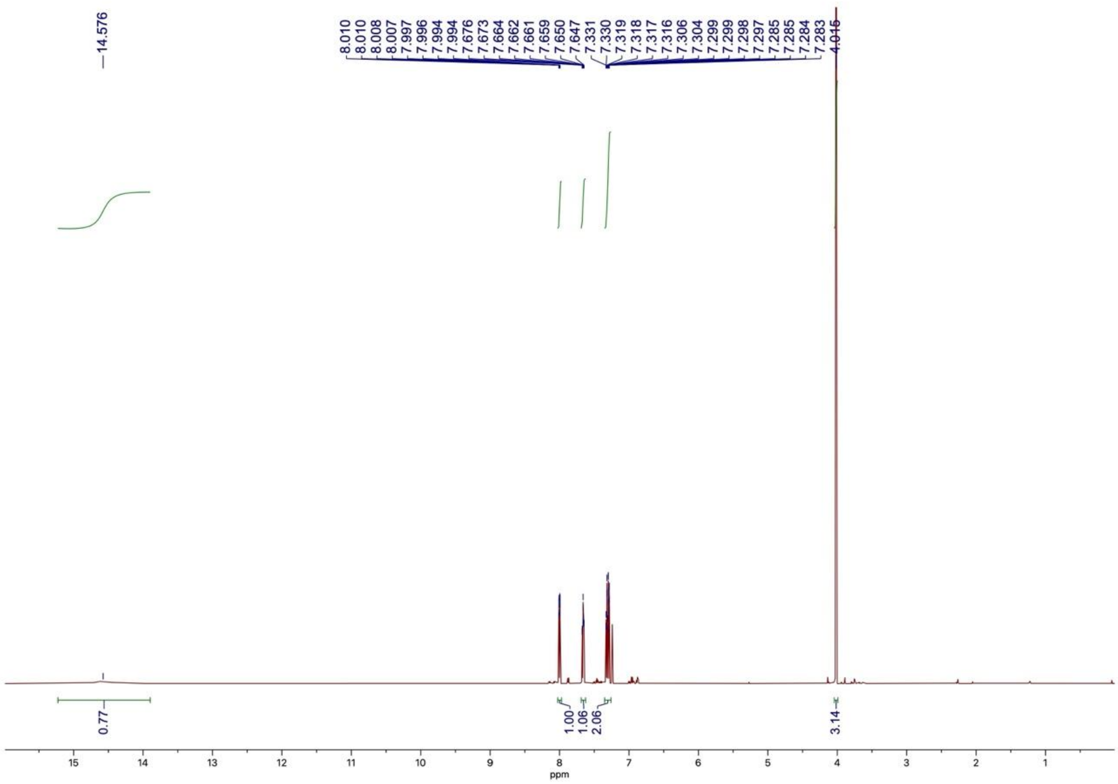

{1H}^{13}C NMR (151 MHz, $CDCl_3$)

Supporting information

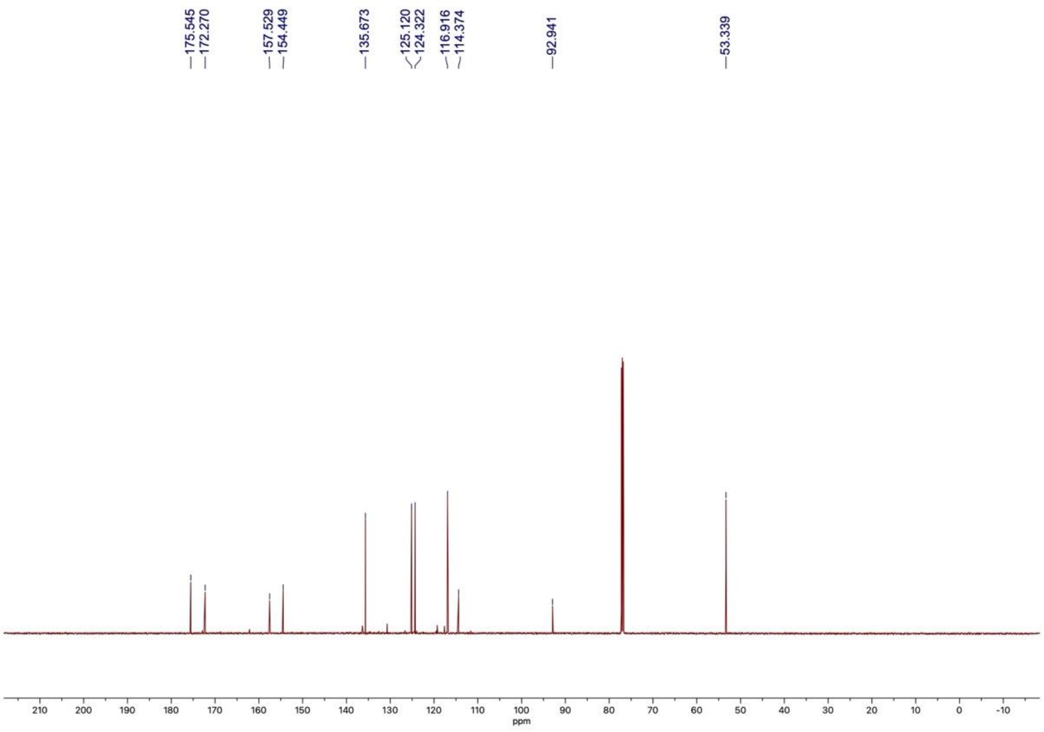

Supporting information

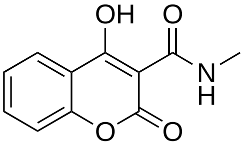

^{1}H NMR (600 MHz, $CDCl_3$)

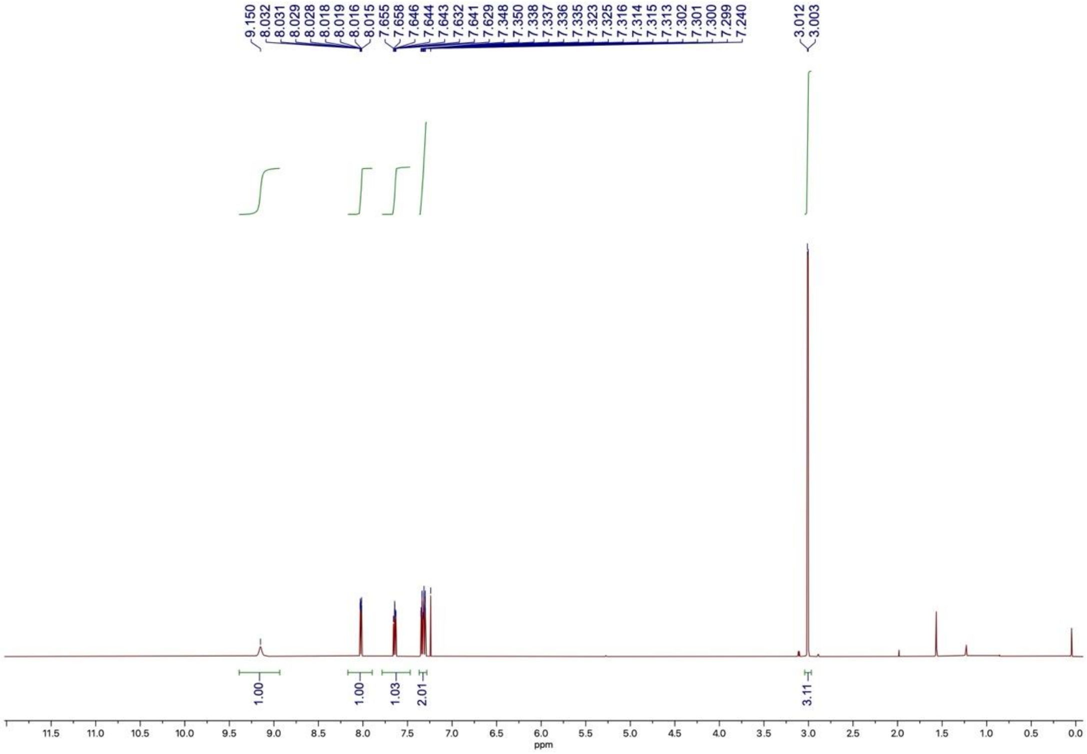

{1H}^{13}C NMR (151 MHz, $CDCl_3$)

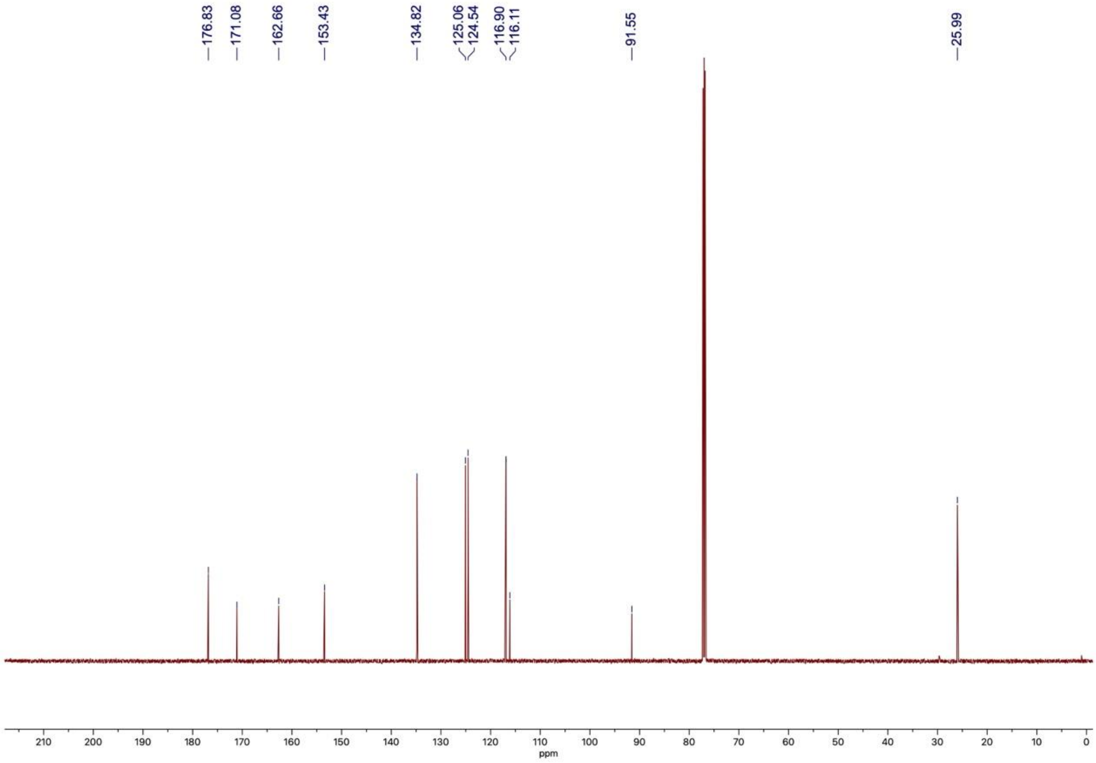
176.83
171.08
162.66
153.43
134.82
125.06
124.54
116.90
116.11
91.55
25.99
210 200 190 180 170 160 150 140 130 120 110 100 90 80 70 60 50 40 30 20 10 0
ppm

Supporting information

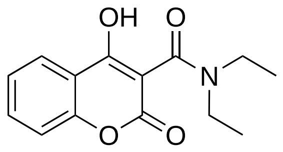

^{1}H NMR (400 MHz, $CDCl_3$)

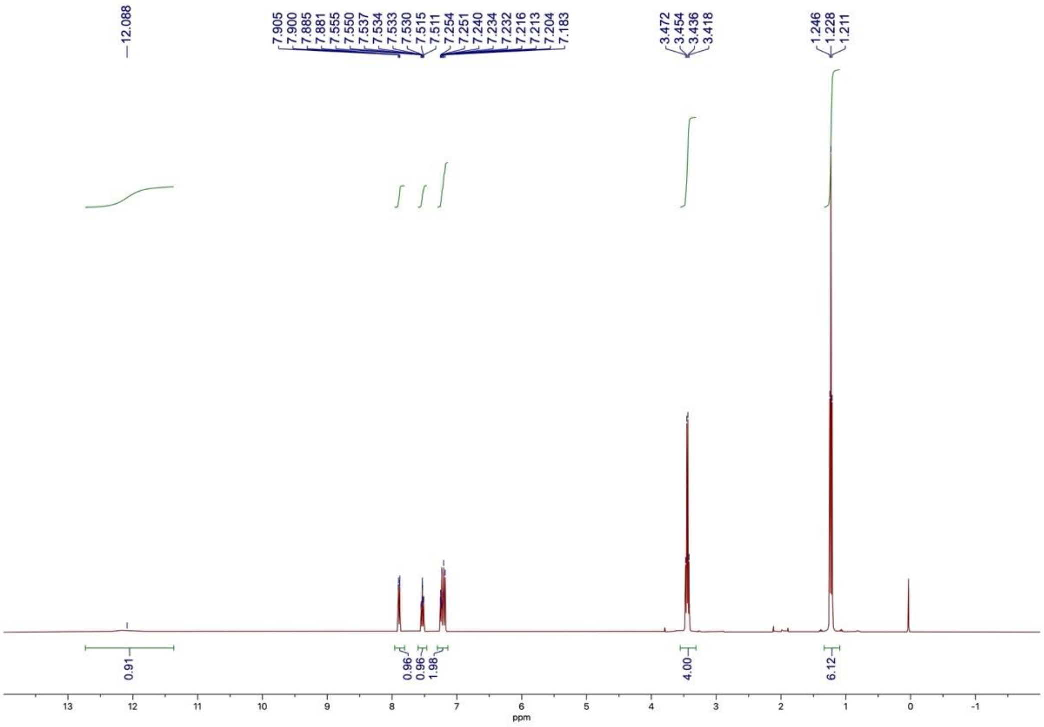

{1H}^{13}C NMR (101 MHz, $CDCl_3$)

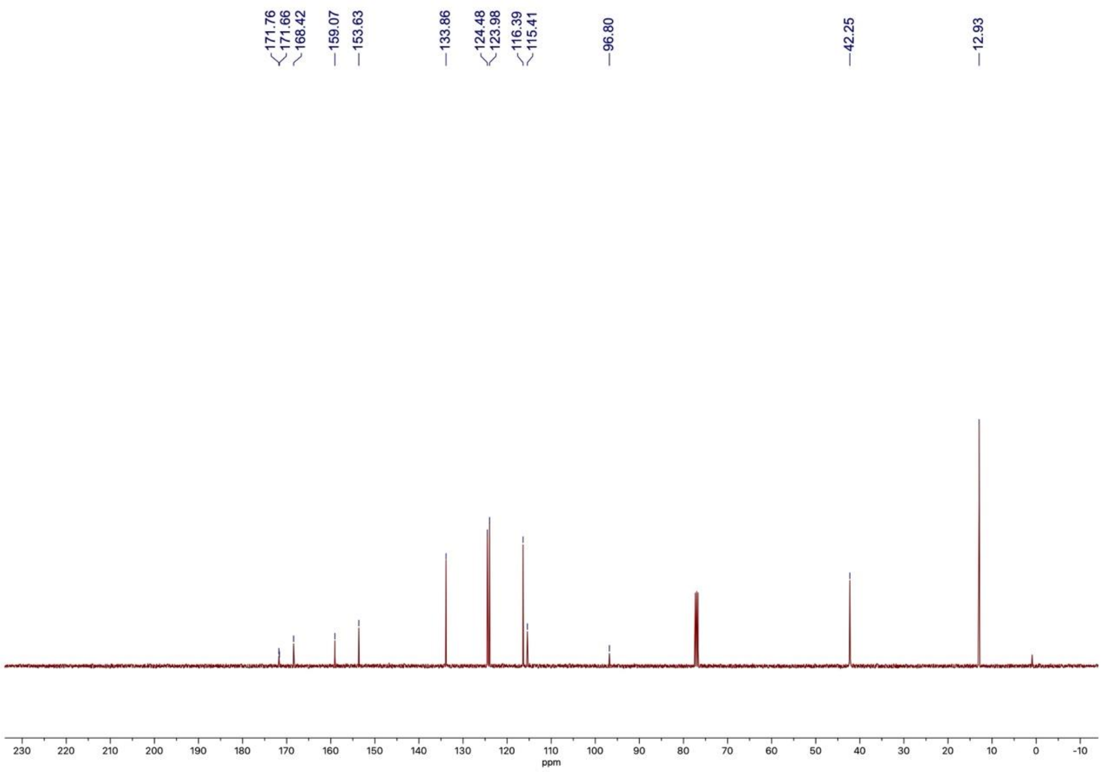
171.76
171.66
168.42
159.07
153.63
133.86
124.48
123.98
116.39
115.41
96.80
42.25
12.93
230 220 210 200 190 180 170 160 150 140 130 120 110 100 90 80 70 60 50 40 30 20 10 0 -10
ppm

Supporting information

1.5. ESI-MS characterization

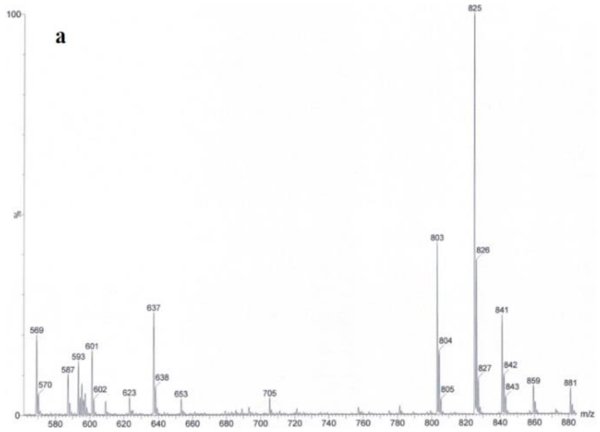

Most relevant signals (m/z)	Corresponding Ions
859	$\{[Tbbpcd(CoumA)][K]H_2O\}^+$
841	$\{[Tbbpcd(CoumA)][K]\}^+$
825	$\{[Tbbpcd(CoumA)][Na]\}^+$
803	$\{[Tbbpcd(CoumA)][H]\}^+$

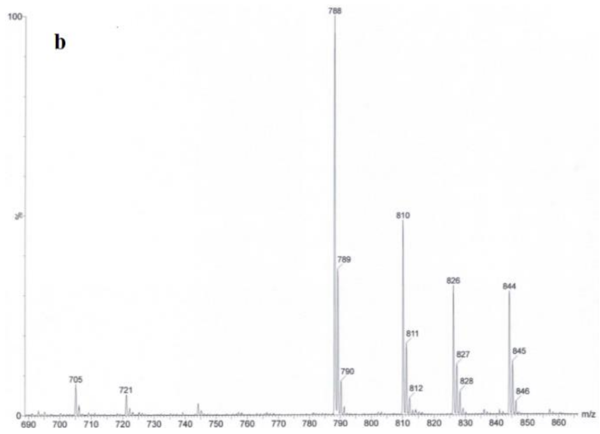

Most relevant signals (m/z)	Corresponding Ions
844	$\{[Tbbpcd(CoumB)][K]H_2O\}^+$
826	$\{[Tbbpcd(CoumB)][K]\}^+$
810	$\{[Tbbpcd(CoumB)][Na]\}^+$
788	$\{[Tbbpcd(CoumB)][H]\}^+$

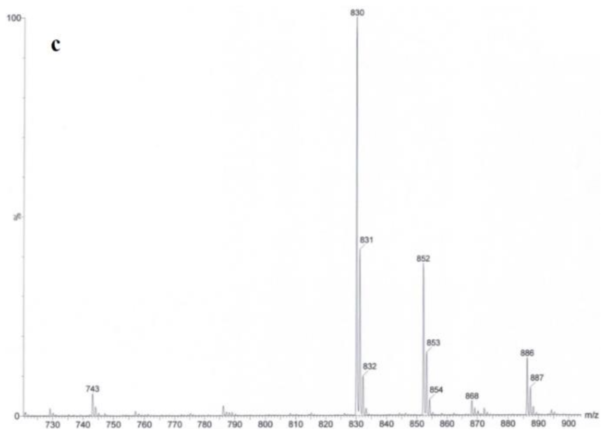

Most relevant signals (m/z)	Corresponding Ions
886	$\{[Tbbpcd(CoumC)][K]H_2O\}^+$
868	$\{[Tbbpcd(CoumC)][K]\}^+$
852	$\{[Tbbpcd(CoumC)][Na]\}^+$
830	$\{[Tbbpcd(CoumC)][H]\}^+$

Figure S1. (Left) ESI-MS spectra of Tb(III)bpcd complexes with: a) Coumarin A, b) Coumarin B and c) Coumarin C and related peaks assignment (right).

Supporting information

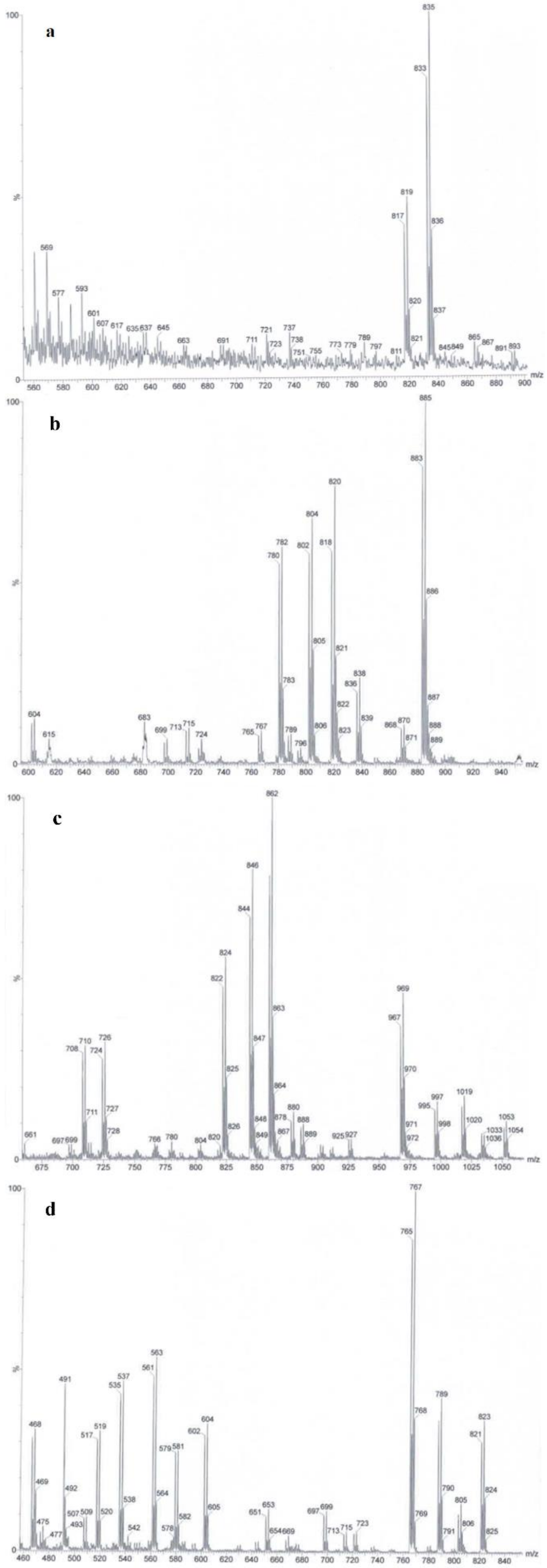

Most relevant signals (m/z)	Corresponding Ions
835	{[Eubpcd(CoumA)][K]}$^+$
819	{[Eubpcd(CoumA)][Na]}$^+$

Most relevant signals (m/z)	Corresponding Ions
885	{[Eubpcd(CoumB)][K][H][MeOH]$_2$}$^+$
820	{[Eubpcd(CoumB)][K]}$^+$
804	{[Eubpcd(CoumB)][Na]}$^+$
782	{[Eubpcd(CoumB)][H]}$^+$

Most relevant signals (m/z)	Corresponding Ions
862	{[Eubpcd(CoumC)][K]}$^+$
846	{[Eubpcd(CoumC)][Na]}$^+$
824	{[Eubpcd(CoumC)][H]}$^+$

Most relevant signals (m/z)	Corresponding Ions
823	{[Eubpcd(Coum)][K]H_2O}$^+$
805	{[Eubpcd(Coum)][K]}$^+$
789	{[Eubpcd(Coum)][Na]}$^+$
767	{[Eubpcd(Coum)][H]}$^+$

Figure S2. (Left) ESI-MS spectra of Eu(III)bpcd complexes with: a) Coumarin A, b) Coumarin B, c) Coumarin C and d) Coumarin and related peaks assignment (right).

Supporting information

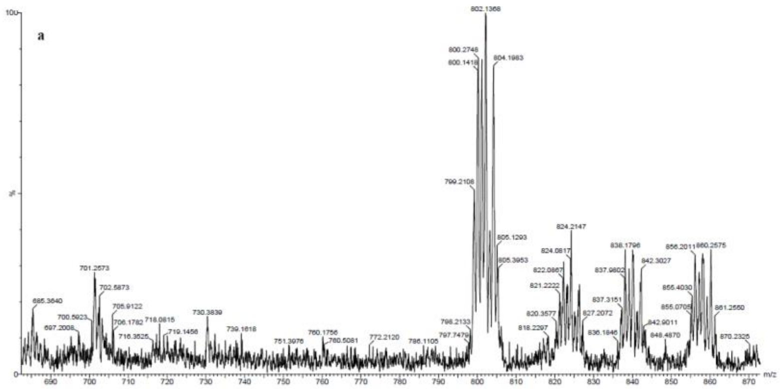

Most relevant signals (m/z)	Corresponding Ions
858	$\{[Gdbpcd(CoumA)][K]H_2O\}^+$
840	$\{[Gdbpcd(CoumA)][K]\}^+$
824	$\{[Gdbpcd(CoumA)][Na]\}^+$
802	$\{[Gdbpcd(CoumA)][H]\}^+$

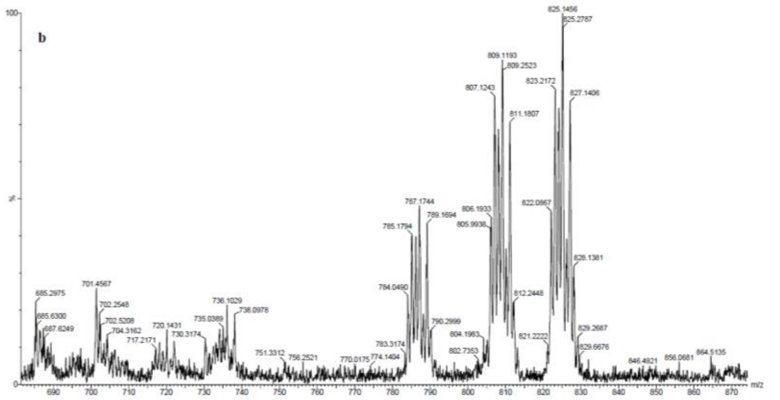

Most relevant signals (m/z)	Corresponding Ions
825	$\{[Gdbpcd(CoumB)][K]\}^+$
809	$\{[Gdbpcd(Coumb)][Na]\}^+$
787	$\{[Gdbpcd(CoumB)][H]\}^+$

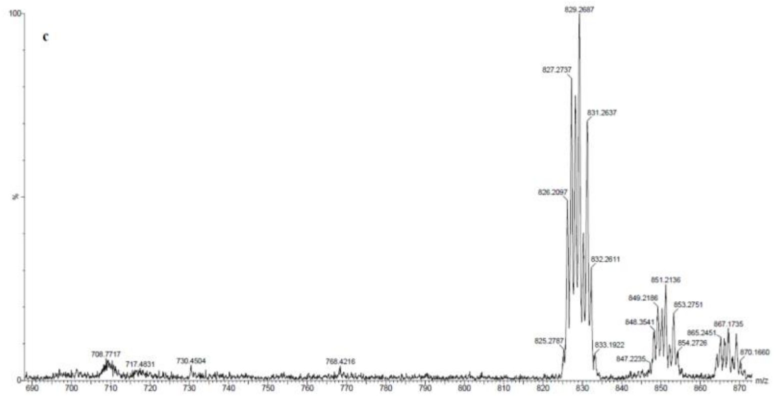

Most relevant signals (m/z)	Corresponding Ions
865	$\{[Gdbpcd(CoumC)][K]\}^+$
849	$\{[Gdbpcd(CoumC)][Na]\}^+$
827	$\{[Gdbpcd(CoumC)][H]\}^+$

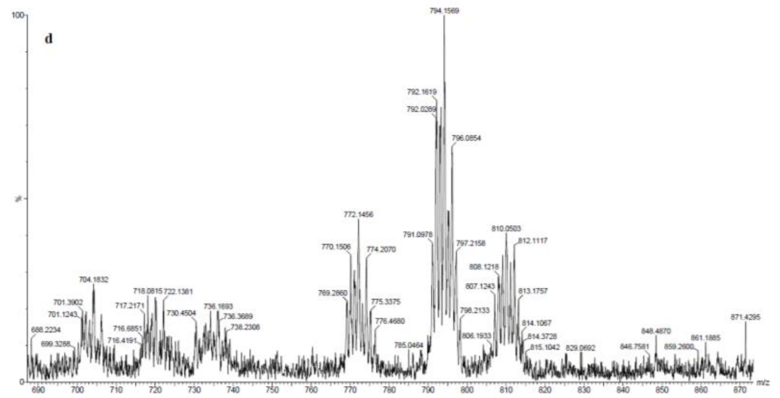

Most relevant signals (m/z)	Corresponding Ions
810	$\{[Gdbpcd(Coum)][K]\}^+$
794	$\{[Gdbpcd(Coum)][Na]\}^+$
772	$\{[Gdbpcd(Coum)][H]\}^+$

Figure S3. (Left) ESI-MS spectra of Gd(III)bpcd complexes with: a) Coumarin A, b) Coumarin B, c) Coumarin C and d) Coumarin and related peaks assignment (right).

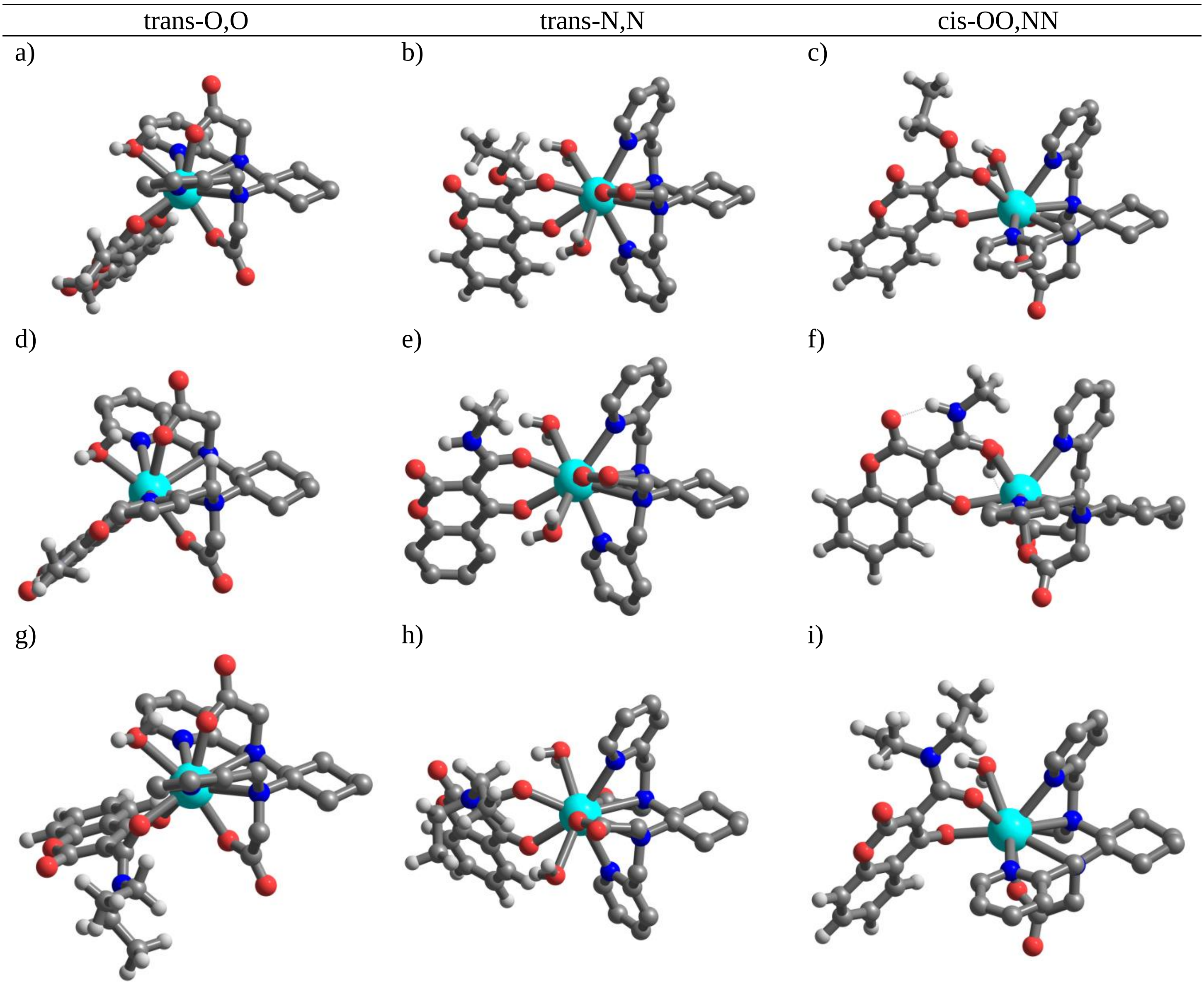

Figure S4. Minimum energy structures of the isomers of the [La(bpcd)(CoumA)(H_2O)$_j$] (a-c), [La(bpcd)(CoumB)(H_2O)$_j$] (d-f) and [La(bpcd)(CoumC)(H_2O)$_j$] (g-i) complexes obtained from DFT calculations. For the *trans*-O,O and *cis*-OO,NN j = 1 while for the *trans*-N,N j = 2. Hydrogen atoms of the Ln(bpcd)$^+$ moieties are hidden for clarity.

1.6. Energy levels diagram

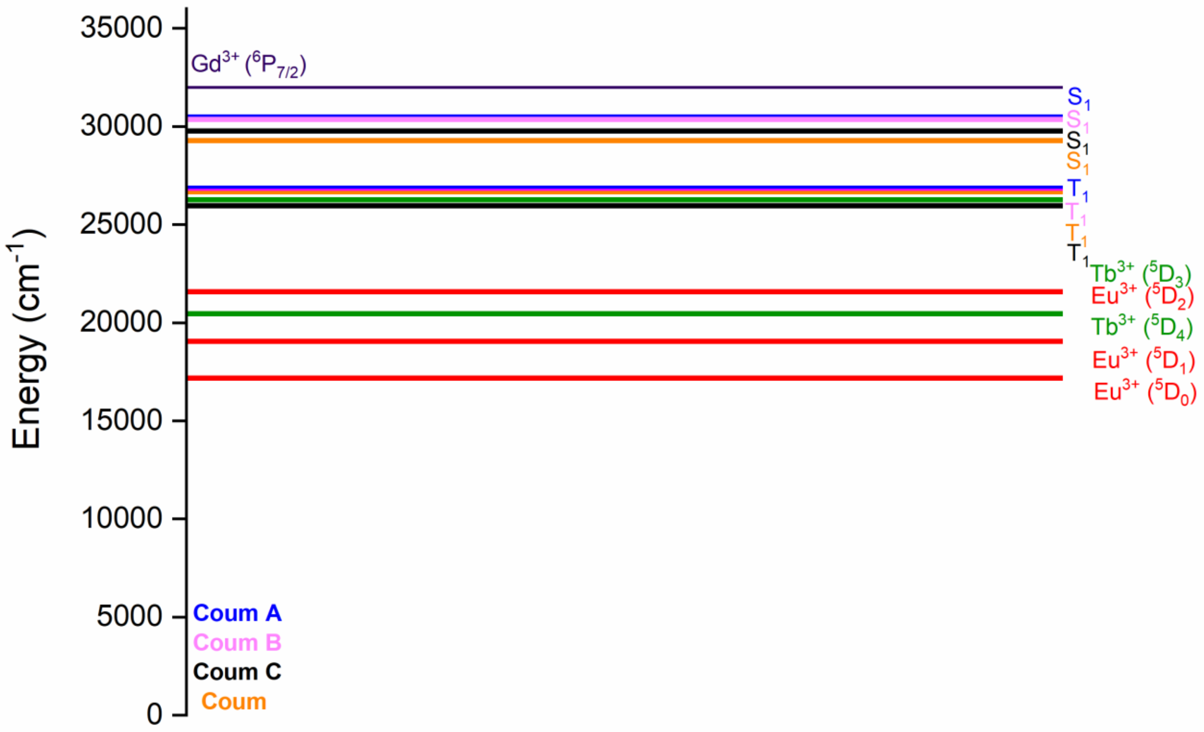

Figure S5. Energy position of S_1 and T_1 levels of the coumarins ligands together with the Tb(III), Gd(III) and Eu(III) levels.

Supporting information

1.7. Luminescence characterization

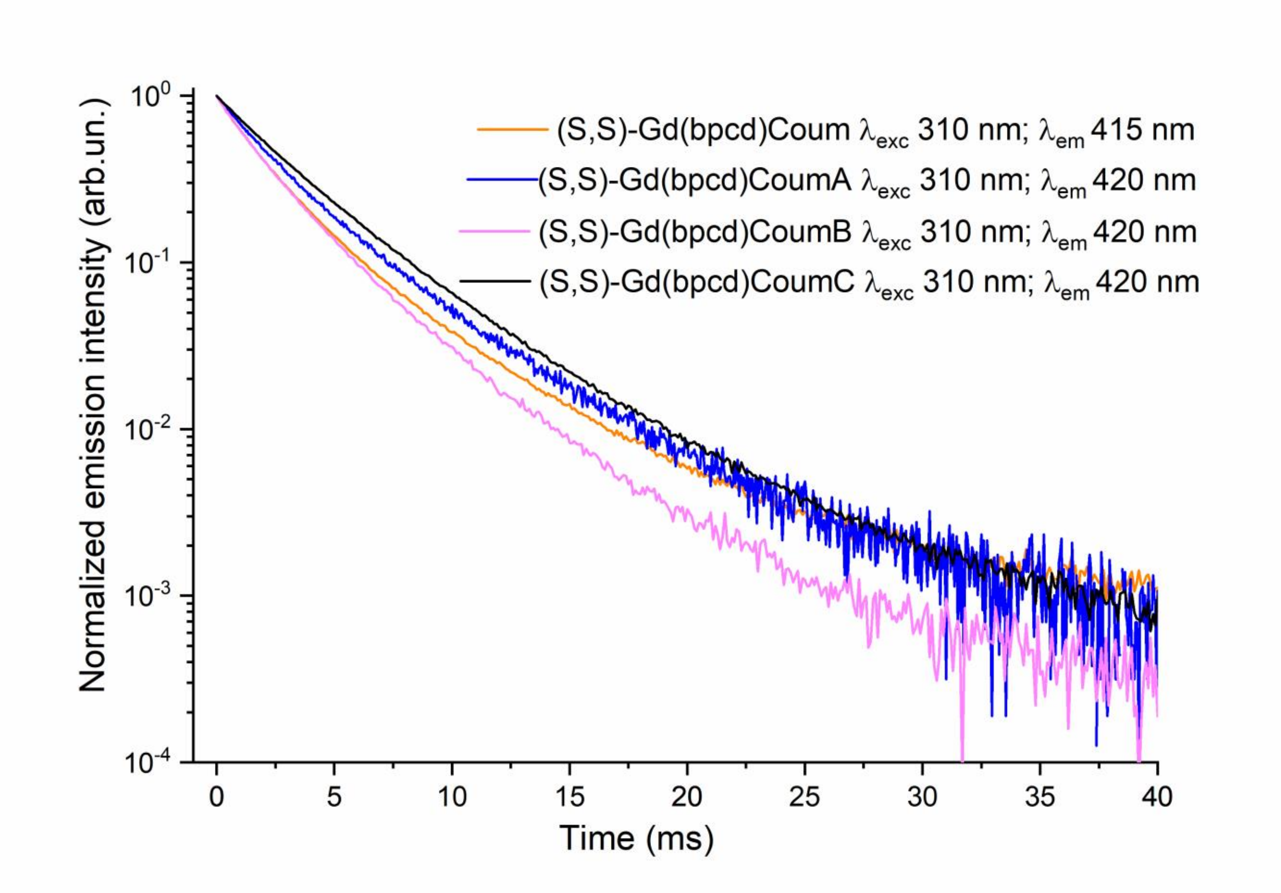

Figure S6. 77 K Luminescence decay curves of the T_1 level for the different coumarins ligands collected upon excitation at 310 nm of the related Gd(III) complexes.

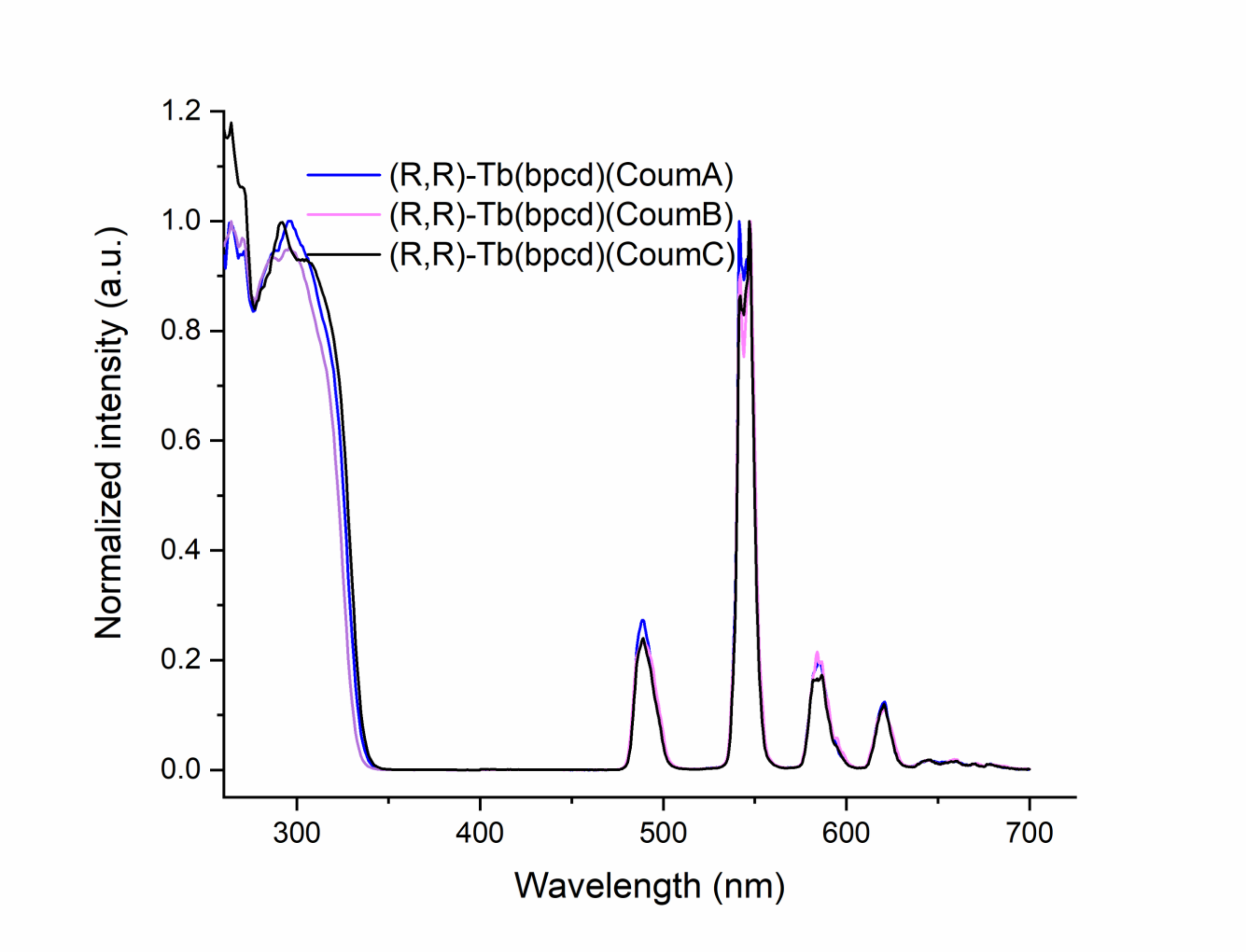

Figure S7. Room temperature excitation (λ_{em} = 546 nm) and emission spectra (λ_{exc} = 300 nm) of (R,R) Tb(III)-based complexes in methanol solution (50 µM).

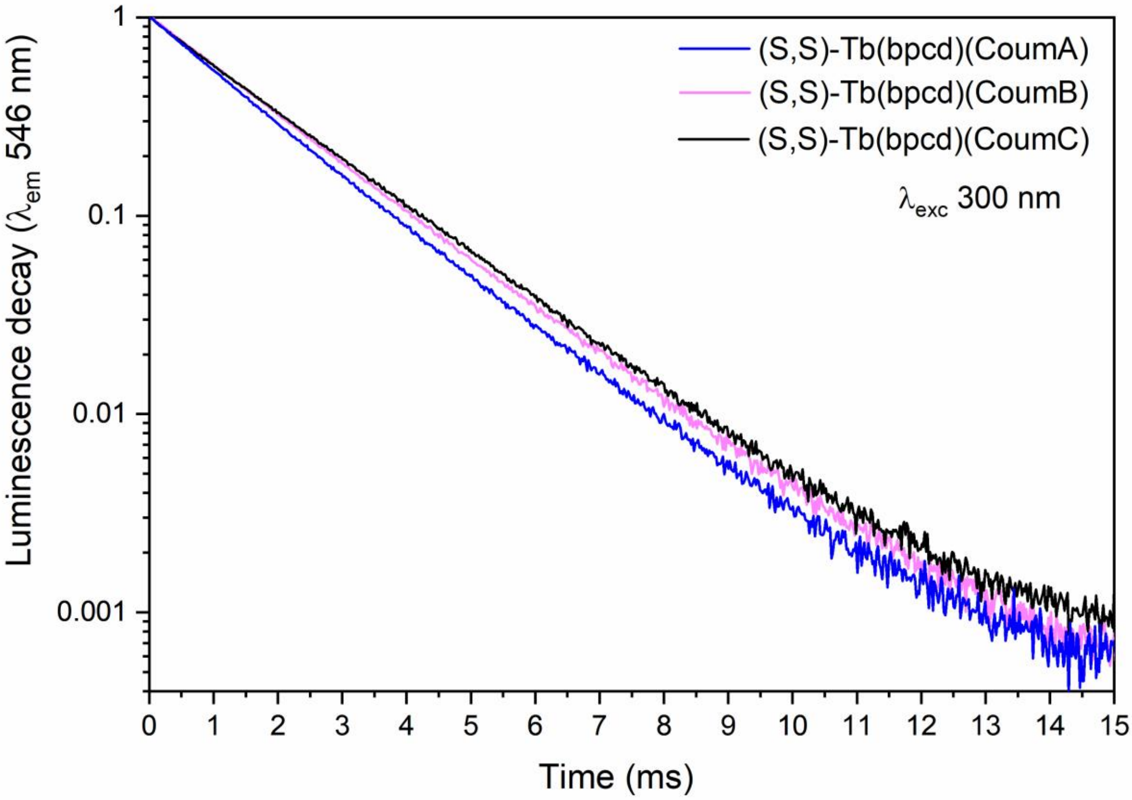

Figure S8. $^5D_4$ excited state decay curves of the different Tb(III) complexes. λ_{exc} 300 nm; λ_{em} 546 nm. All curves can be fitted by an exponential function, from which τ_{obs} can be determined.

1.8. CPL activity

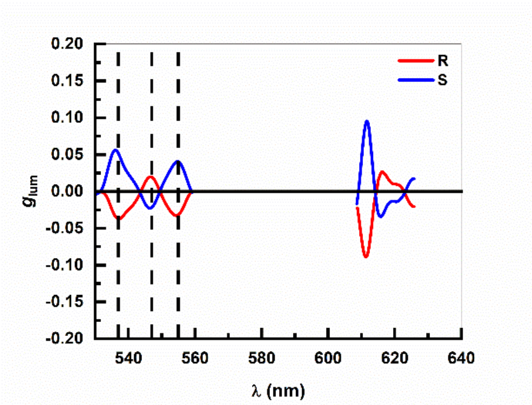

Figure S9. [Tb(bpcd)(Coum)]; A plot of g_{lum} vs. wavelength of the two enantiomers. The dashed lines indicate the three maxima for the $^5D_4 \rightarrow {}^7F_5$ transition. The g_{lum} values for the $^5D_4 \rightarrow {}^7F_J$ (J = 4,3) transitions are also shown.

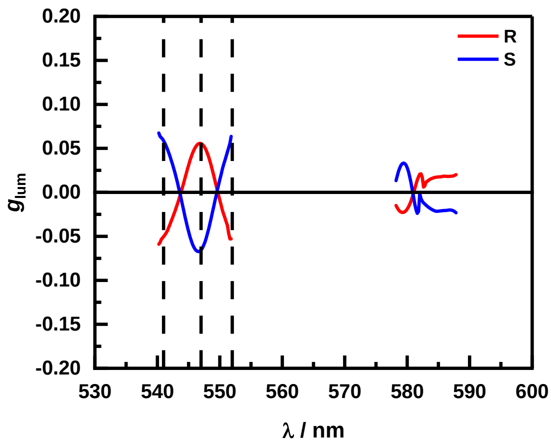

Figure S10. [Tb(bpcd)(CoumA)]; A plot of g_{lum} vs. wavelength of the two enantiomers. The dashed lines indicate the three maxima for the $^5D_4 \rightarrow {}^7F_5$ transition. The g_{lum} values for the $^5D_4 \rightarrow {}^7F_3$ transition between 575 and 590 nm are also shown.

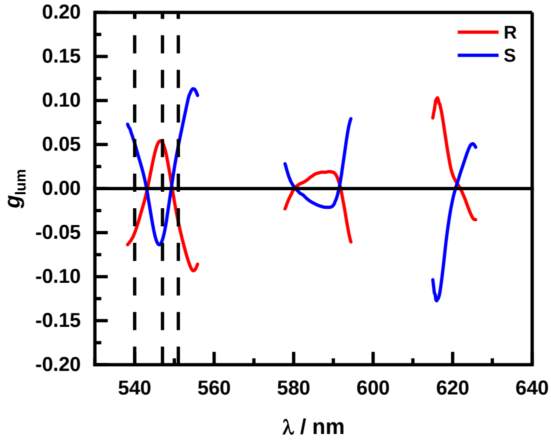

Figure S11. [Tb(bpcd)(CoumB)]; A plot of g_{lum} vs. wavelength of the two enantiomers. The dashed lines indicate the three maxima for the $^5D_4 \rightarrow {}^7F_5$ transition. The g_{lum} values for the $^5D_4 \rightarrow {}^7F_J$ (J = 4,3) transitions are also shown.

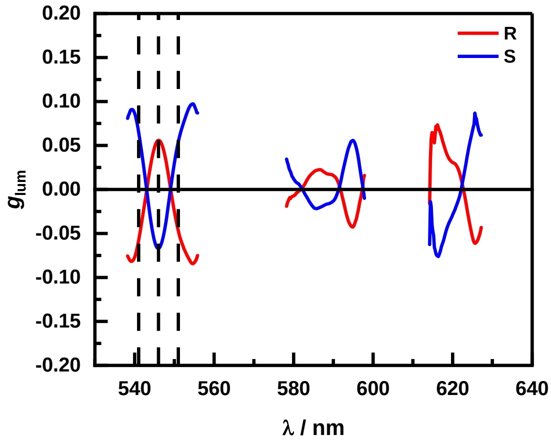

Figure S12. [Tb(bpcd)(CoumC)]; A plot of g_{lum} vs. wavelength of the two enantiomers. The dashed lines indicate the three maxima for the $^5D_4 \rightarrow {}^7F_5$ transition. The g_{lum} values for the $^5D_4 \rightarrow {}^7F_J$ (J = 4,3) transitions are also shown.

Supporting information

2. Chiroptical instrumentation

2.1. CPL measurements

Discrimination of left/right circular polarized states was performed by a photoelastic modulator from a decommissioned Jasco J500C spectropolarimeter operating at 50 KHz coupled with an uncoated Glenn-Thompson polarizer. A Jasco CT-10 was used as the emission monochromator and the detection was performed by a Hamamatsu R376 PMT. The spectra were collected under either 365 or 254 nm irradiation from commercial LED-sources, using a 90° geometry between the excitation and detection direction. All CPL spectra were recorded in 1 cm semi-micro (aperture 4 mm) optical glass cells using the following parameters: scan-speed 0.5 nm/sec, integration time 2 sec, photomultiplier tube driving voltage 600 V, accumulations 4.

2.2. UV-Vis/ECD measurements

UV-Vis spectra were recorded using a Jasco-V650 spectrophotometer in the spectral range of 200 to 400 nm. All samples were measured in 1 mM MeOH solutions at room temperature. The same solutions were used to record CD spectra using a J1500 spectropolarimeter in 0.01 cm optical glass cells.

Given the complex structure of CPL spectra with several opposite bands within the same manifold, a more general definition of B_{CPL} factor was employed:

$$B_{CPL} = \varepsilon \cdot \varphi \cdot \frac{1}{2} \frac{\int_{\lambda_a}^{\lambda_b} I(\lambda) g(\lambda) d\lambda}{\int_{\lambda_i}^{\lambda_f} I(\lambda) d\lambda} \tag{S1}$$

where the integral in the numerator has to be estimated between the extrema of the considered transition (λ_a, λ_b), while the integral in the denominator is calculated over the whole emission range (λ_i, λ_f). Note that if $g(\lambda)$ does not change sign within a term-to-term transition and it is approximately constant ($g(\lambda) \simeq \bar{g}$), then the above definition is reduced to:

$$B_{CPL} = \varepsilon \cdot \varphi \cdot \frac{1}{2} \bar{g} \cdot \frac{\int_{\lambda_a}^{\lambda_b} I(\lambda) d\lambda}{\int_{\lambda_i}^{\lambda_f} I(\lambda) d\lambda} = \varepsilon \cdot \varphi \cdot \frac{1}{2} \bar{g} \cdot \beta \tag{S2}$$

According to the usual definition applicable to lanthanide CPL.[S1]

Supporting information

3. Theoretical modeling

3.1. Intramolecular energy transfer rates

The intramolecular energy transfer (IET) rates from ligands to the Ln(III) were calculated considering the dipole-dipole (W_{d-d}), dipole-multipole (W_{d-m}), and exchange (W_{ex}) mechanisms:[4–8]

$$W_{d-d} = \frac{S_L(1-\sigma_1)^2}{(2J+1)G}\frac{4\pi}{\hbar}\frac{e^2}{R_L^6}\sum_{\lambda}\Omega_\lambda^{FED}\langle\psi'J'\|U^{(\lambda)}\|\psi J\rangle^2 F \quad \text{(S3)}$$

$$W_{d-m} = \frac{S_L}{(2J+1)G}\frac{2\pi e^2}{\hbar}\sum_{\lambda}(\lambda+1)\times\frac{\langle r^\lambda\rangle^2}{\left(R_L^{\lambda+2}\right)^2}\langle f\|C^{(\lambda)}\|f\rangle^2(1-\sigma_\lambda)^2\langle\psi'J'\|U^{(\lambda)}\|\psi J\rangle^2 F \quad \text{(S4)}$$

$$W_{ex} = \frac{(1-\sigma_0)^2}{(2J+1)G}\frac{8\pi}{\hbar}\frac{e^2}{R_L^4}\langle\psi'J'\|S\|\psi J\rangle^2\sum_m\left|\langle\phi\right|\textstyle\sum_j\mu_z(j)s_m(j)\left|\phi^*\rangle\right|^2 F \quad \text{(S5)}$$

where Ω_λ^{FED} are the intensity parameters taking into account only the FED mechanism and these quantities were estimated using the Simple Overlap model [9,10] in the JOYSpectra platform [11], accessed through http://www.joyspectra.website. The values of the squared reduced matrix elements $\langle\psi'J'\|U^{(\lambda)}\|\psi J\rangle^2$ were taken from Carnall's tables.[12] S_L is the dipole strength of the ligand transition involved in IET (10^{-36} and 10^{-40} $(esu)^2\cdot cm^2$ for S_1 and T_1, respectively [8]), $\langle r^\lambda\rangle$ are the $4f$ radial integrals, G is the ligand state degeneracy ($G = 1$ or 3 for S_1 or T_1, respectively), $\langle f\|C^{(\lambda)}\|f\rangle$ is the reduced matrix element of Racah's tensor operators, and $(1-\sigma_k)$ are the shielding factors which have a relation with the overlap integrals between valence orbitals of the pair Ln–O.[7,13]

In the exchange mechanism (Eq. S5), s_m is the spin operator in the ligand and μ_z is the projection of the dipole operator on the z-component, the value of the element matrix of these coupled operators is $\sim 10^{-36}$ $(esu)^2\cdot cm^2$.[8,14] The $\langle\psi'J'\|S\|\psi J\rangle$ is the reduced matrix elements of the spin operator, which were calculated using free-ion wavefunctions in the intermediate coupling scheme.[15,16]

The donor-acceptor states distances (R_L) are estimated from the TD-DFT calculations, as illustrated in terms of molecular orbitals compositions of the excited states S_1 and T_1 as illustrated in Figure S13 and the R_L is the centroid of these compositions (Figure S14).

The term F in Eqs. S3–S5 represents the spectral overlap factor, accounting for the energy mismatch condition between the donor and acceptor states.[4,8] For ligand-to-metal energy transfer, F can be estimated using the following equation:

Supporting information

$$F = \frac{G(\Delta, T)}{\hbar\gamma_L}\sqrt{\frac{\ln(2)}{\pi}}\, e^{-\left(\frac{\Delta}{\hbar\gamma_L}\right)^2 \ln(2)} \tag{S6}$$

with Δ being the energy difference between the donor state (i.e., the barycenter energy of the S_1 or T_1) of and lanthanide ion acceptor state (i.e., Eu^{3+} $^5D_1$ or Tb^{3+} $^5D_4$), $\Delta = E_D - E_{Ln}$. The γ_L is the bandwidth at half-height for the donor state, assumed here a typical value of $\gamma_L = 4000$ cm^{-1} for S_1 states. G(Δ,T) represents the energy barrier, which considers the energy mismatch between donor and acceptor. If Δ is negative, meaning the donor energy is lower than the energy of the acceptor, then $G(\Delta, T) = exp(\Delta/k_B T)$; however, in the condition of $\Delta \geq 0$, $G(\Delta, T) = 1$. Here, k_B denotes the Boltzmann constant, and T refers to the temperature, which is assumed to be 300 K in this study.

The energy transfer rate for a given pathway (W) is calculated by the sum over Eqs. S3–S5:

$$W = W_{d-d} + W_{d-m} + W_{ex} \tag{S7}$$

All calculated forward and backward IET rates for [Ln(bpcd)X(H_2O)] (Ln = Eu^{3+} and Tb^{3+} and X = CoumA and CoumB) are presented in Tables S1 to S8.

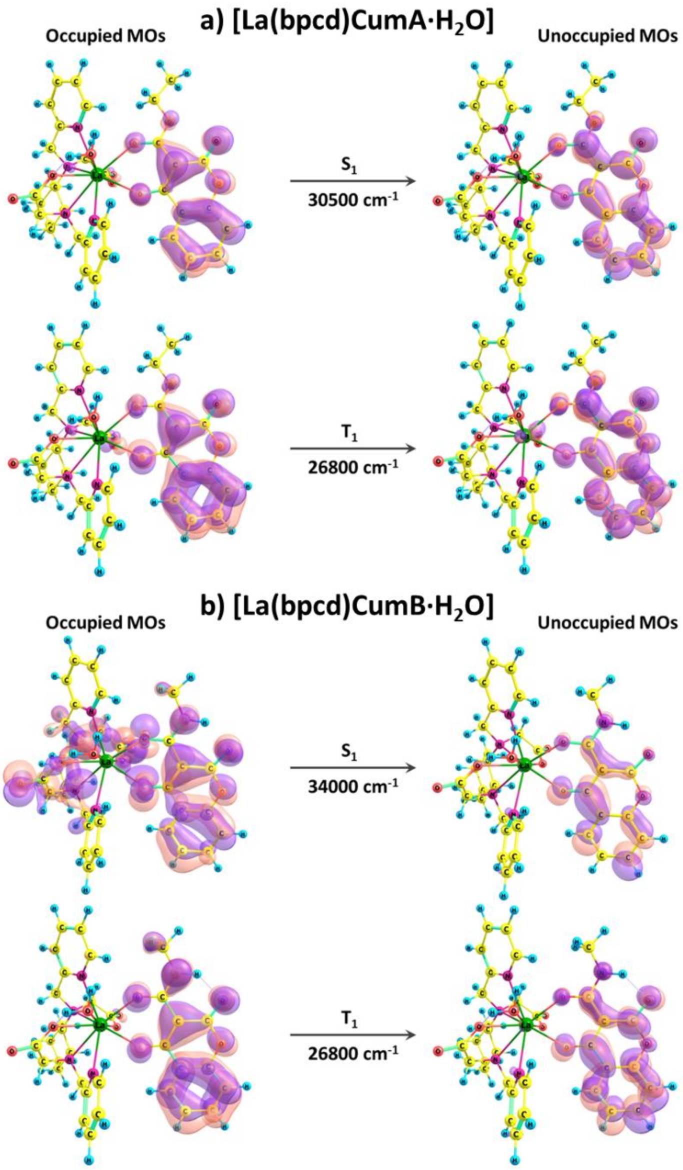

Figure S13. Molecular orbitals compositions of the excited states of a) [La(bpcd)(CoumA)(H_2O)] and b) [La(bpcd)(CoumB)(H_2O)].

Supporting information

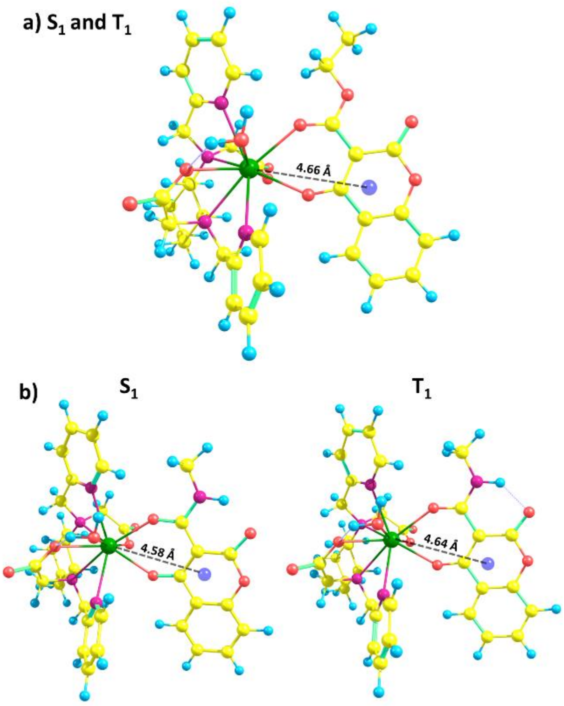

Figure S14. Calculated donor-acceptor distances for the excited states of a) CoumA and b) CoumB compounds.

Tables S1–S8 present the energy transfer rates calculated using the JOYSpectra web platform [11] (http://www.joyspectra.website). In these tables, Δ represents the donor–acceptor energy difference between donor and acceptor transitions. W_{d-d}, W_{d-m}, and W_{ex} denote the energy transfer by the dipole–dipole, dipole–multipole, and exchange mechanisms, respectively. W is the sum of all mechanisms for a given pathway (p). The forward (ligand-to-Ln) rates perspective, W^S represents the sum over W involving the S_1 as a donor, while W^T is the sum over W involving the T_1 as a donor state. From the backward (Ln-to-ligand) rates, W_b^S is the sum over W_b involving the S_1 as an acceptor, while W_b^T is the sum over W_b involving the T_1 as the acceptor state.

Supporting information

Table S1. Forward (ligand−to−Eu) IET rates for **[Eu(bpcd)(CoumA)(H_2O)]**.

p	donor	acceptor	contr. (%)	Δ (cm^{-1})	W (s^{-1})	W_{d-d} (s^{-1})	W_{d-m} (s^{-1})	W_{ex} (s^{-1})
1	$S_1 \to S_0$	$^7F_0 \to {}^5D_0$	0.0	13194	2.0×10^{3}	4.2×10^{-1}	2.0×10^{3}	0.0
2	$S_1 \to S_0$	$^7F_0 \to {}^5D_1$	18.9	11460	2.1×10^{6}	0.0	0.0	2.1×10^{6}
3	$S_1 \to S_0$	$^7F_0 \to {}^5D_2$	0.0	9004	0.0	0.0	0.0	0.0
4	$S_1 \to S_0$	$^7F_0 \to {}^5L_6$	0.8	5162	8.9×10^{4}	8.5×10^{4}	3.1×10^{3}	0.0
5	$S_1 \to S_0$	$^7F_0 \to {}^5G_6$	0.3	3735	3.7×10^{4}	3.6×10^{4}	1.3×10^{3}	0.0
6	$S_1 \to S_0$	$^7F_0 \to {}^5D_4$	0.8	2901	8.4×10^{4}	8.5×10^{3}	7.5×10^{4}	0.0
7	$S_1 \to S_0$	$^7F_1 \to {}^5D_0$	0.5	13566	6.1×10^{4}	0.0	0.0	6.1×10^{4}
8	$S_1 \to S_0$	$^7F_1 \to {}^5D_1$	0.1	11832	1.5×10^{4}	3.1	1.5×10^{4}	9.9×10^{1}
9	$S_1 \to S_0$	$^7F_1 \to {}^5D_2$	1.4	9376	1.5×10^{5}	0.0	0.0	1.5×10^{5}
10	$S_1 \to S_0$	$^7F_1 \to {}^5D_3$	1.5	6504	1.6×10^{5}	1.8×10^{2}	1.6×10^{5}	0.0
11	$S_1 \to S_0$	$^7F_1 \to {}^5L_6$	0.0	5534	2.9×10^{3}	2.8×10^{3}	1.0×10^{2}	0.0
12	$S_1 \to S_0$	$^7F_1 \to {}^5L_7$	0.1	4502	9.2×10^{3}	8.8×10^{3}	3.2×10^{2}	0.0
13	$S_1 \to S_0$	$^7F_1 \to {}^5G_2$	73.4	4467	8.2×10^{6}	0.0	0.0	8.2×10^{6}
14	$S_1 \to S_0$	$^7F_1 \to {}^5G_3$	2.1	4237	2.3×10^{5}	4.6×10^{2}	2.3×10^{5}	0.0
15	$S_1 \to S_0$	$^7F_1 \to {}^5G_6$	0.0	4107	2.9×10^{3}	2.8×10^{3}	1.0×10^{2}	0.0
16	$S_1 \to S_0$	$^7F_1 \to {}^5G_5$	0.1	4096	7.1×10^{3}	5.7×10^{3}	1.5×10^{3}	0.0
				W^S	1.1×10^{7}			
17	$T_1 \to S_0$	$^7F_0 \to {}^5D_0$	0.0	6920	1.6×101	3.3×10^{-3}	1.6×10^{1}	0.0
18	$T_1 \to S_0$	$^7F_0 \to {}^5D_1$	89.7	5186	6.5×107	0.0	0.0	6.5×10^{7}
19	$T_1 \to S_0$	$^7F_0 \to {}^5D_2$	0.0	2730	0.0	0.0	0.0	0.0
20	$T_1 \to S_0$	$^7F_0 \to {}^5L_6$	0.0	−1112	4.1×10−2	4.0×10^{-2}	1.5×10^{-3}	0.0
21	$T_1 \to S_0$	$^7F_0 \to {}^5G_6$	0.0	−2539	8.2×10−6	7.9×10^{-6}	2.9×10^{-7}	0.0
22	$T_1 \to S_0$	$^7F_0 \to {}^5D_4$	0.0	−3373	2.1×10−7	2.1×10^{-8}	1.9×10^{-7}	0.0
23	$T_1 \to S_0$	$^7F_1 \to {}^5D_0$	8.2	7292	5.9×106	0.0	0.0	5.9×10^{6}
24	$T_1 \to S_0$	$^7F_1 \to {}^5D_1$	0.0	5558	3.8×103	1.2×10^{-2}	5.5×10^{1}	3.7×10^{3}
25	$T_1 \to S_0$	$^7F_1 \to {}^5D_2$	2.1	3102	1.5×106	0.0	0.0	1.5×10^{6}
26	$T_1 \to S_0$	$^7F_1 \to {}^5D_3$	0.0	230	3.4×101	3.7×10^{-2}	3.4×10^{1}	0.0
27	$T_1 \to S_0$	$^7F_1 \to {}^5L_6$	0.0	−740	1.0×10−2	9.8×10^{-3}	3.6×10^{-4}	0.0
28	$T_1 \to S_0$	$^7F_1 \to {}^5L_7$	0.0	−1772	1.2×10−4	1.2×10^{-4}	4.3×10^{-6}	0.0
29	$T_1 \to S_0$	$^7F_1 \to {}^5G_2$	0.0	−1807	9.2×102	0.0	0.0	9.2×10^{2}
30	$T_1 \to S_0$	$^7F_1 \to {}^5G_3$	0.0	−2037	7.7×10−4	1.5×10^{-6}	7.6×10^{-4}	0.0
31	$T_1 \to S_0$	$^7F_1 \to {}^5G_6$	0.0	−2167	4.7×10−6	4.5×10^{-6}	1.6×10^{-7}	0.0
32	$T_1 \to S_0$	$^7F_1 \to {}^5G_5$	0.0	−2178	1.1×10−5	8.7×10^{-6}	2.2×10^{-6}	0.0
				W^T	6.6×10^{7}			
				$W^{T'}$	5.9×10^{6}			

Supporting information

Table S2. Backward (Eu−to−ligand) IET rates for **[Eu(bpcd)(CoumA)(H_2O)]**.

p	donor	acceptor	contr. (%)	Δ (cm^{-1})	W_b (s^{-1})	W_{d-d} (s^{-1})	W_{d-m} (s^{-1})	W_{ex} (s^{-1})
1	$^5D_0\rightarrow^7F_0$	$S_0\rightarrow S_1$	0.0	−13194	5.4×10^{-25}	1.1×10^{-28}	5.4×10^{-25}	0.0
2	$^5D_1\rightarrow^7F_0$	$S_0\rightarrow S_1$	0.0	−11460	8.1×10^{-19}	0.0	0.0	8.1×10^{-19}
3	$^5D_2\rightarrow^7F_0$	$S_0\rightarrow S_1$	0.0	−9004	0.0	0.0	0.0	0.0
4	$^5L_6\rightarrow^7F_0$	$S_0\rightarrow S_1$	0.0	−5162	1.2×10^{-7}	1.2×10^{-7}	4.4×10^{-9}	0.0
5	$^5G_6\rightarrow^7F_0$	$S_0\rightarrow S_1$	0.2	−3735	5.1×10^{-5}	4.9×10^{-5}	1.8×10^{-6}	0.0
6	$^5D_4\rightarrow^7F_0$	$S_0\rightarrow S_1$	40.4	−2901	9.3×10^{-3}	9.5×10^{-4}	8.4×10^{-3}	0.0
7	$^5D_0\rightarrow^7F_1$	$S_0\rightarrow S_1$	0.0	−13566	4.1×10^{-23}	0.0	0.0	4.1×10^{-23}
8	$^5D_1\rightarrow^7F_1$	$S_0\rightarrow S_1$	0.0	−11832	1.4×10^{-20}	3.0×10^{-24}	1.4×10^{-20}	9.5×10^{-23}
9	$^5D_2\rightarrow^7F_1$	$S_0\rightarrow S_1$	0.0	−9376	1.2E$\times10^{-14}$	0.0	0.0	1.2×10^{-14}
10	$^5D_3\rightarrow^7F_1$	$S_0\rightarrow S_1$	0.0	−6504	9.8×10^{-9}	1.1×10^{-11}	9.8×10^{-9}	0.0
11	$^5L_6\rightarrow^7F_1$	$S_0\rightarrow S_1$	0.0	−5534	1.0×10^{-8}	1.0×10^{-8}	3.6×10^{-10}	0.0
12	$^5L_7\rightarrow^7F_1$	$S_0\rightarrow S_1$	0.0	−4502	4.1×10^{-6}	3.9×10^{-6}	1.4×10^{-7}	0.0
13	$^5G_2\rightarrow^7F_1$	$S_0\rightarrow S_1$	55.8	−4467	1.3×10^{-2}	0.0	0.0	1.3×10^{-2}
14	$^5G_3\rightarrow^7F_1$	$S_0\rightarrow S_1$	3.5	−4237	8.0×10^{-4}	1.6×10^{-6}	8.0×10^{-4}	0.0
15	$^5G_6\rightarrow^7F_1$	$S_0\rightarrow S_1$	0.0	−4107	9.9×10^{-6}	9.5×10^{-6}	3.5×10^{-7}	0.0
16	$^5G_5\rightarrow^7F_1$	$S_0\rightarrow S_1$	0.1	−4096	3.1×10^{-5}	2.4×10^{-5}	6.3×10^{-6}	0.0
				W_b^S	2.3×10^{-2}			
17	$^5D_0\rightarrow^7F_0$	$S_0\rightarrow T_1$	0.0	−6920	6.0×10^{-14}	1.3×10^{-17}	6.0×10^{-14}	0.0
18	$^5D_1\rightarrow^7F_0$	$S_0\rightarrow T_1$	0.0	−5186	3.5×10^{-4}	0.0	0.0	3.5×10^{-4}
19	$^5D_2\rightarrow^7F_0$	$S_0\rightarrow T_1$	0.0	−2730	0.0	0.0	0.0	0.0
20	$^5L_6\rightarrow^7F_0$	$S_0\rightarrow T_1$	0.0	1112	8.2×10^{-1}	7.9×10^{-1}	2.9×10^{-2}	0.0
21	$^5G_6\rightarrow^7F_0$	$S_0\rightarrow T_1$	0.0	2539	1.6×10^{-1}	1.5×10^{-1}	5.5×10^{-3}	0.0
22	$^5D_4\rightarrow^7F_0$	$S_0\rightarrow T_1$	0.0	3373	3.3×10^{-1}	3.3×10^{-2}	2.9×10^{-1}	0.0
23	$^5D_0\rightarrow^7F_1$	$S_0\rightarrow T_1$	0.0	−7292	5.6×10^{-8}	0.0	0.0	5.6×10^{-8}
24	$^5D_1\rightarrow^7F_1$	$S_0\rightarrow T_1$	0.0	−5558	5.1×10^{-8}	1.6×10^{-13}	7.4×10^{-10}	5.1×10^{-8}
25	$^5D_2\rightarrow^7F_1$	$S_0\rightarrow T_1$	0.0	−3102	1.7	0.0	0.0	1.7
26	$^5D_3\rightarrow^7F_1$	$S_0\rightarrow T_1$	0.0	−230	2.9×10^{1}	3.1×10^{-2}	2.9×10^{1}	0.0
27	$^5L_6\rightarrow^7F_1$	$S_0\rightarrow T_1$	0.0	740	5.0×10^{-1}	4.8×10^{-1}	1.8×10^{-2}	0.0
28	$^5L_7\rightarrow^7F_1$	$S_0\rightarrow T_1$	0.0	1772	7.7×10^{-1}	7.5×10^{-1}	2.7×10^{-2}	0.0
29	$^5G_2\rightarrow^7F_1$	$S_0\rightarrow T_1$	100.0	1807	2.0×10^{7}	0.0	0.0	2.0×10^{7}
30	$^5G_3\rightarrow^7F_1$	$S_0\rightarrow T_1$	0.0	2037	3.7×10^{1}	7.2×10^{-2}	3.7×10^{1}	0.0
31	$^5G_6\rightarrow^7F_1$	$S_0\rightarrow T_1$	0.0	2167	2.3×10^{-1}	2.2×10^{-1}	7.9×10^{-3}	0.0
32	$^5G_5\rightarrow^7F_1$	$S_0\rightarrow T_1$	0.0	2178	6.6×10^{-1}	5.2×10^{-1}	1.4×10^{-1}	0.0
				W_b^T	2.0×10^{7}			
				$W_b^{T'}$	5.8×10^{-8}			

Supporting information

Table S3. Forward (ligand−to−Eu) IET rates for **[Eu(bpcd)(CoumB)(H_2O)]**.

p	donor	acceptor	contr. (%)	Δ (cm^{-1})	W (s^{-1})	W_{d-d} (s^{-1})	W_{d-m} (s^{-1})	W_{ex} (s^{-1})
1	$S_1 \to S_0$	$^7F_0 \to {}^5D_0$	0.0	13067	2.5×10^{3}	5.9×10^{-1}	2.5×10^{3}	0.0
2	$S_1 \to S_0$	$^7F_0 \to {}^5D_1$	20.2	11333	2.9×10^{6}	0.0	0.0	2.9×10^{6}
3	$S_1 \to S_0$	$^7F_0 \to {}^5D_2$	0.0	8877	0.0	0.0	0.0	0.0
4	$S_1 \to S_0$	$^7F_0 \to {}^5L_6$	0.7	5035	9.3×10^{4}	8.9×10^{4}	4.3×10^{3}	0.0
5	$S_1 \to S_0$	$^7F_0 \to {}^5G_6$	0.3	3608	3.8×10^{4}	3.7×10^{4}	1.8×10^{3}	0.0
6	$S_1 \to S_0$	$^7F_0 \to {}^5D_4$	0.7	2774	1.0×10^{5}	8.8×10^{3}	9.6×10^{4}	0.0
7	$S_1 \to S_0$	$^7F_1 \to {}^5D_0$	0.6	13439	8.6×10^{4}	0.0	0.0	8.6×10^{4}
8	$S_1 \to S_0$	$^7F_1 \to {}^5D_1$	0.1	11705	1.8×10^{4}	4.3	1.8×10^{4}	1.4×10^{2}
9	$S_1 \to S_0$	$^7F_1 \to {}^5D_2$	1.4	9249	2.1×10^{5}	0.0	0.0	2.1×10^{5}
10	$S_1 \to S_0$	$^7F_1 \to {}^5D_3$	1.3	6377	1.9×10^{5}	2.0×10^{2}	1.9×10^{5}	0.0
11	$S_1 \to S_0$	$^7F_1 \to {}^5L_6$	0.0	5407	3.1×10^{3}	3.0×10^{3}	1.4×10^{2}	0.0
12	$S_1 \to S_0$	$^7F_1 \to {}^5L_7$	0.1	4375	9.6×10^{3}	9.1×10^{3}	4.4×10^{2}	0.0
13	$S_1 \to S_0$	$^7F_1 \to {}^5G_2$	72.6	4340	1.0×10^{7}	0.0	0.0	1.0×10^{7}
14	$S_1 \to S_0$	$^7F_1 \to {}^5G_3$	1.8	4110	2.6×10^{5}	4.9×10^{2}	2.6×10^{5}	0.0
15	$S_1 \to S_0$	$^7F_1 \to {}^5G_6$	0.0	3980	3.0×10^{3}	2.9×10^{3}	1.4×10^{2}	0.0
16	$S_1 \to S_0$	$^7F_1 \to {}^5G_5$	0.1	3969	7.7×10^{3}	5.8×10^{3}	1.9×10^{3}	0.0
				$\boldsymbol{W^S}$	1.4×10^{7}			
17	$T_1 \to S_0$	$^7F_0 \to {}^5D_0$	0.0	6630	1.8×10^{1}	4.4×10^{-3}	1.8×10^{1}	0.0
18	$T_1 \to S_0$	$^7F_0 \to {}^5D_1$	89.4	4896	7.7×10^{7}	0.0	0.0	7.7×10^{7}
19	$T_1 \to S_0$	$^7F_0 \to {}^5D_2$	0.0	2440	0.0	0.0	0.0	0.0
20	$T_1 \to S_0$	$^7F_0 \to {}^5L_6$	0.0	−1402	9.1×10^{-3}	8.7×10^{-3}	3.7×10^{-4}	0.0
21	$T_1 \to S_0$	$^7F_0 \to {}^5G_6$	0.0	−2829	1.7×10^{-6}	1.7×10^{-6}	7.1×10^{-8}	0.0
22	$T_1 \to S_0$	$^7F_0 \to {}^5D_4$	0.0	−3663	4.9×10^{-8}	4.5×10^{-9}	4.5×10^{-8}	0.0
23	$T_1 \to S_0$	$^7F_1 \to {}^5D_0$	8.6	7002	7.4×10^{6}	0.0	0.0	7.4×10^{6}
24	$T_1 \to S_0$	$^7F_1 \to {}^5D_1$	0.0	5268	4.5×10^{3}	1.5×10^{-2}	6.0×10^{1}	4.5×10^{3}
25	$T_1 \to S_0$	$^7F_1 \to {}^5D_2$	2.0	2812	1.7×10^{6}	0.0	0.0	1.7×10^{6}
26	$T_1 \to S_0$	$^7F_1 \to {}^5D_3$	0.0	−60	2.4×10^{1}	2.6×10^{-2}	2.4×10^{1}	0.0
27	$T_1 \to S_0$	$^7F_1 \to {}^5L_6$	0.0	−1030	2.2×10^{-3}	2.2×10^{-3}	9.2×10^{-5}	0.0
28	$T_1 \to S_0$	$^7F_1 \to {}^5L_7$	0.0	−2062	2.7×10^{-5}	2.6×10^{-5}	1.1×10^{-6}	0.0
29	$T_1 \to S_0$	$^7F_1 \to {}^5G_2$	0.0	−2097	2.3×10^{2}	0.0	0.0	2.3×10^{2}
30	$T_1 \to S_0$	$^7F_1 \to {}^5G_3$	0.0	−2327	1.7×10^{-4}	3.3×10^{-7}	1.7×10^{-4}	0.0
31	$T_1 \to S_0$	$^7F_1 \to {}^5G_6$	0.0	−2457	1.0×10^{-6}	9.5×10^{-7}	4.1×10^{-8}	0.0
32	$T_1 \to S_0$	$^7F_1 \to {}^5G_5$	0.0	−2468	2.4×10^{-6}	1.8×10^{-6}	5.5×10^{-7}	0.0
				$\boldsymbol{W^T}$	7.9×10^{7}			
				$\boldsymbol{W^{T'}}$	7.4×10^{6}			

Table S4. Backward (Eu−to−ligand) IET rates for **[Eu(bpcd)(CoumB)(H_2O)]**.

p	donor	acceptor	contr. (%)	Δ (cm^{-1})	W_b (s^{-1})	W_{d-d} (s^{-1})	W_{d-m} (s^{-1})	W_{ex} (s^{-1})
1	$^5D_0 \to {}^7F_0$	$S_0 \to S_1$	0.0	−13067	1.2×10^{-24}	2.9×10^{-28}	1.2×10^{-24}	0.0
2	$^5D_1 \to {}^7F_0$	$S_0 \to S_1$	0.0	−11333	2.1×10^{-18}	0.0	0.0	2.1×10^{-18}
3	$^5D_2 \to {}^7F_0$	$S_0 \to S_1$	0.0	−8877	0.0	0.0	0.0	0.0
4	$^5L_6 \to {}^7F_0$	$S_0 \to S_1$	0.0	−5035	2.4×10^{-7}	2.3×10^{-7}	1.1×10^{-8}	0.0
5	$^5G_6 \to {}^7F_0$	$S_0 \to S_1$	0.2	−3608	9.7×10^{-5}	9.3×10^{-5}	4.5×10^{-6}	0.0
6	$^5D_4 \to {}^7F_0$	$S_0 \to S_1$	40.1	−2774	2.1×10^{-2}	1.8×10^{-3}	2.0×10^{-2}	0.0
7	$^5D_0 \to {}^7F_1$	$S_0 \to S_1$	0.0	−13439	1.1×10^{-22}	0.0	0.0	1.1×10^{-22}
8	$^5D_1 \to {}^7F_1$	$S_0 \to S_1$	0.0	−11705	3.2×10^{-20}	7.5×10^{-24}	3.1×10^{-20}	2.4×10^{-22}
9	$^5D_2 \to {}^7F_1$	$S_0 \to S_1$	0.0	−9249	3.1×10^{-14}	0.0	0.0	3.1×10^{-14}
10	$^5D_3 \to {}^7F_1$	$S_0 \to S_1$	0.0	−6377	2.1×10^{-8}	2.2×10^{-11}	2.1×10^{-8}	0.0
11	$^5L_6 \to {}^7F_1$	$S_0 \to S_1$	0.0	−5407	2.0×10^{-8}	1.9×10^{-8}	9.4×10^{-10}	0.0
12	$^5L_7 \to {}^7F_1$	$S_0 \to S_1$	0.0	−4375	7.8×10^{-6}	7.5×10^{-6}	3.6×10^{-7}	0.0
13	$^5G_2 \to {}^7F_1$	$S_0 \to S_1$	56.4	−4340	3.0×10^{-2}	0.0	0.0	3.0×10^{-2}
14	$^5G_3 \to {}^7F_1$	$S_0 \to S_1$	3.1	−4110	1.6×10^{-3}	3.1×10^{-6}	1.6×10^{-3}	0.0
15	$^5G_6 \to {}^7F_1$	$S_0 \to S_1$	0.0	−3980	1.9×10^{-5}	1.8×10^{-5}	8.8×10^{-7}	0.0
16	$^5G_5 \to {}^7F_1$	$S_0 \to S_1$	0.1	−3969	6.1×10^{-5}	4.6×10^{-5}	1.5×10^{-5}	0.0
				W_b^S	5.3×10^{-2}			
17	$^5D_0 \to {}^7F_0$	$S_0 \to T_1$	0.0	−6630	2.7×10^{-13}	6.8×10^{-17}	2.7×10^{-13}	0.0
18	$^5D_1 \to {}^7F_0$	$S_0 \to T_1$	0.0	−4896	1.7×10^{-3}	0.0	0.0	1.7×10^{-3}
19	$^5D_2 \to {}^7F_0$	$S_0 \to T_1$	0.0	−2440	0.0	0.0	0.0	0.0
20	$^5L_6 \to {}^7F_0$	$S_0 \to T_1$	0.0	1402	7.3×10^{-1}	7.0×10^{-1}	3.0×10^{-2}	0.0
21	$^5G_6 \to {}^7F_0$	$S_0 \to T_1$	0.0	2829	1.4×10^{-1}	1.3×10^{-1}	5.5×10^{-3}	0.0
22	$^5D_4 \to {}^7F_0$	$S_0 \to T_1$	0.0	3663	3.1×10^{-1}	2.8×10^{-2}	2.8×10^{-1}	0.0
23	$^5D_0 \to {}^7F_1$	$S_0 \to T_1$	0.0	−7002	2.8×10^{-7}	0.0	0.0	2.8×10^{-7}
24	$^5D_1 \to {}^7F_1$	$S_0 \to T_1$	0.0	−5268	2.5×10^{-7}	8.2×10^{-13}	3.3×10^{-9}	2.5×10^{-7}
25	$^5D_2 \to {}^7F_1$	$S_0 \to T_1$	0.0	−2812	8.0	0.0	0.0	8.0
26	$^5D_3 \to {}^7F_1$	$S_0 \to T_1$	0.0	60	8.4×10^{1}	9.1×10^{-2}	8.3×10^{1}	0.0
27	$^5L_6 \to {}^7F_1$	$S_0 \to T_1$	0.0	1030	4.5×10^{-1}	4.3×10^{-1}	1.8×10^{-2}	0.0
28	$^5L_7 \to {}^7F_1$	$S_0 \to T_1$	0.0	2062	6.7×10^{-1}	6.5×10^{-1}	2.8×10^{-2}	0.0
29	$^5G_2 \to {}^7F_1$	$S_0 \to T_1$	100.0	2097	2.0×10^{7}	0.0	0.0	2.0×10^{7}
30	$^5G_3 \to {}^7F_1$	$S_0 \to T_1$	0.0	2327	3.3×10^{1}	6.4×10^{-2}	3.3×10^{1}	0.0
31	$^5G_6 \to {}^7F_1$	$S_0 \to T_1$	0.0	2457	1.9×10^{-1}	1.9×10^{-1}	8.0×10^{-3}	0.0
32	$^5G_5 \to {}^7F_1$	$S_0 \to T_1$	0.0	2468	5.8×10^{-1}	4.5×10^{-1}	1.3×10^{-1}	0.0
				W_b^T	2.0×10^{7}			
				$W_b^{T'}$	2.8×10^{-7}			

Supporting information

Table S5. Forward (ligand−to−Tb) IET rates for **[Tb(bpcd)(CoumA)(H_2O)]**.

p	donor	acceptor	contr. (%)	Δ (cm^{-1})	W (s^{-1})	W_{d-d} (s^{-1})	W_{d-m} (s^{-1})	W_{ex} (s^{-1})
1	$S_1 \rightarrow S_0$	$^7F_6 \rightarrow ^5D_4$	0.0	10043	3.8×10^4	2.9×10^1	3.8×10^4	0.0
2	$S_1 \rightarrow S_0$	$^7F_6 \rightarrow ^5D_3$	0.0	4251	1.3×10^3	7.3×10^2	5.8×10^2	0.0
3	$S_1 \rightarrow S_0$	$^7F_6 \rightarrow ^5G_6$	59.5	4064	6.6×10^8	6.1×10^4	2.6×10^6	6.6×10^8
4	$S_1 \rightarrow S_0$	$^7F_6 \rightarrow ^5L_{10}$	0.0	3516	3.8×10^4	3.6×10^4	2.2×10^3	0.0
5	$S_1 \rightarrow S_0$	$^7F_6 \rightarrow ^5G_5$	6.3	2720	7.0×10^7	1.1×10^4	2.9×10^6	6.7×10^7
6	$S_1 \rightarrow S_0$	$^7F_6 \rightarrow ^5G_4$	0.0	2200	2.8×10^5	7.6×10^3	2.7×10^5	0.0
7	$S_1 \rightarrow S_0$	$^7F_6 \rightarrow ^5L_9$	0.0	2079	5.1×10^4	4.0×10^4	1.1×10^4	0.0
8	$S_1 \rightarrow S_0$	$^7F_6 \rightarrow ^5G_3$	0.0	1510	2.6×10^3	1.4×10^3	1.1×10^3	0.0
9	$S_1 \rightarrow S_0$	$^7F_6 \rightarrow ^5L_8$	0.0	1297	2.3×10^4	2.2×10^4	1.3×10^3	0.0
10	$S_1 \rightarrow S_0$	$^7F_6 \rightarrow ^5L_7$	0.2	1030	1.9×10^6	1.2×10^4	1.9×10^6	9.0×10^2
11	$S_1 \rightarrow S_0$	$^7F_6 \rightarrow ^5L_6$	1.9	817	2.1×10^7	0.0	0.0	2.1×10^7
12	$S_1 \rightarrow S_0$	$^7F_6 \rightarrow ^5H_7$	0.0	−892	3.2×10^5	0.0	0.0	3.2×10^5
13	$S_1 \rightarrow S_0$	$^7F_6 \rightarrow ^5H_6$	0.0	−2404	1.4×10^3	0.0	0.0	1.4×10^3
14	$S_1 \rightarrow S_0$	$^7F_6 \rightarrow ^5H_5$	0.0	−3280	1.8×10^{-7}	0.0	0.0	1.8×10^{-7}
15	$S_1 \rightarrow S_0$	$^7F_6 \rightarrow ^5F_5$	0.0	−4447	8.1×10^{-2}	0.0	0.0	8.1×10^{-2}
16	$S_1 \rightarrow S_0$	$^7F_6 \rightarrow ^5I_7$	0.0	−6102	5.7×10^{-7}	0.0	0.0	5.7×10^{-7}
17	$S_1 \rightarrow S_0$	$^7F_6 \rightarrow ^5I_6$	0.0	−7111	3.6×10^{-8}	0.0	0.0	3.6×10^{-8}
18	$S_1 \rightarrow S_0$	$^7F_6 \rightarrow ^5I_5$	0.0	−7499	3.6×10^{-10}	0.0	0.0	3.6×10^{-10}
19	$S_1 \rightarrow S_0$	$^7F_6 \rightarrow ^5K_5$	0.0	−10847	1.3×10^{-19}	0.0	0.0	1.3×10^{-19}
20	$S_1 \rightarrow S_0$	$^7F_6 \rightarrow ^5K_7$	0.0	−11206	1.9×10^{-27}	0.0	0.0	1.9×10^{-27}
21	$S_1 \rightarrow S_0$	$^7F_5 \rightarrow ^5D_4$	0.0	12091	3.6×10^5	1.9×10^1	9.8×10^4	2.6×10^5
22	$S_1 \rightarrow S_0$	$^7F_5 \rightarrow ^5D_3$	0.0	6299	3.5×10^5	8.2×10^2	3.5×10^5	0.0
23	$S_1 \rightarrow S_0$	$^7F_5 \rightarrow ^5G_6$	4.0	6112	4.4×10^7	3.1×10^3	3.1×10^6	4.1×10^7
24	$S_1 \rightarrow S_0$	$^7F_5 \rightarrow ^5L_{10}$	0.0	5564	5.0×10^2	4.8×10^2	1.6×10^1	0.0
25	$S_1 \rightarrow S_0$	$^7F_5 \rightarrow ^5G_5$	23.4	4768	2.6×10^8	3.1×10^3	1.5×10^5	2.6×10^8
26	$S_1 \rightarrow S_0$	$^7F_5 \rightarrow ^5D_2$	0.0	4428	9.6×10^3	1.3×10^3	8.3×10^3	0.0
27	$S_1 \rightarrow S_0$	$^7F_5 \rightarrow ^5G_4$	3.7	4248	4.1×10^7	1.3×10^3	8.9×10^5	4.0×10^7
28	$S_1 \rightarrow S_0$	$^7F_5 \rightarrow ^5L_9$	0.0	4127	1.1×10^4	8.3×10^3	2.7×10^3	0.0
29	$S_1 \rightarrow S_0$	$^7F_5 \rightarrow ^5L_8$	0.0	3345	2.6×10^4	1.7×10^4	8.9×10^3	0.0
30	$S_1 \rightarrow S_0$	$^7F_5 \rightarrow ^5L_7$	0.0	3078	5.3×10^5	5.6×10^3	5.2×10^5	0.0
31	$S_1 \rightarrow S_0$	$^7F_5 \rightarrow ^5I_6$	0.2	2865	2.4×10^6	0.0	0.0	2.4×10^6
32	$S_1 \rightarrow S_0$	$^7F_5 \rightarrow ^5H_6$	0.5	−356	5.3×10^6	0.0	0.0	5.3×10^6
33	$S_1 \rightarrow S_0$	$^7F_5 \rightarrow ^5H_5$	0.1	−1232	9.1×10^5	0.0	0.0	9.1×10^5
34	$S_1 \rightarrow S_0$	$^7F_5 \rightarrow ^5H_4$	0.0	−1804	1.2×10^5	0.0	0.0	1.2×10^5
35	$S_1 \rightarrow S_0$	$^7F_5 \rightarrow ^5F_5$	0.0	−2399	3.6×10^3	0.0	0.0	3.6×10^3
36	$S_1 \rightarrow S_0$	$^7F_5 \rightarrow ^5F_4$	0.0	−2839	1.2×10^3	0.0	0.0	1.2×10^3
37	$S_1 \rightarrow S_0$	$^7F_5 \rightarrow ^5I_6$	0.0	−5063	3.7×10^{-4}	0.0	0.0	3.7×10^{-4}
38	$S_1 \rightarrow S_0$	$^7F_5 \rightarrow ^5I_4$	0.0	−5073	3.5×10^{-7}	0.0	0.0	3.5×10^{-7}
39	$S_1 \rightarrow S_0$	$^7F_5 \rightarrow ^5I_5$	0.0	−5451	3.2×10^{-6}	0.0	0.0	3.2×10^{-6}
40	$S_1 \rightarrow S_0$	$^7F_5 \rightarrow ^5K_5$	0.0	−8799	1.1×10^{-14}	0.0	0.0	1.1×10^{-14}
				W^S	1.1×10^9			
41	$T_1 \rightarrow S_0$	$^7F_6 \rightarrow ^5D_4$	0.0	3769	5.4×10^1	4.1×10^{-2}	5.4×10^1	0.0

42	$T_1 \to S_0$	$^7F_6 \to {}^5D_3$	0.0	−2023	4.6×10^{-6}	2.6×10^{-6}	2.0×10^{-6}	0.0
43	$T_1 \to S_0$	$^7F_6 \to {}^5G_6$	0.0	−2210	8.5×10^{3}	7.9×10^{-5}	3.3×10^{-3}	8.5×10^{3}
44	$T_1 \to S_0$	$^7F_6 \to {}^5L_{10}$	0.0	−2758	2.6×10^{-6}	2.4×10^{-6}	1.5×10^{-7}	0.0
45	$T_1 \to S_0$	$^7F_6 \to {}^5G_5$	0.0	−3554	6.3×10^{-1}	1.1×10^{-8}	2.7×10^{-6}	6.3×10^{-1}
46	$T_1 \to S_0$	$^7F_6 \to {}^5G_4$	0.0	−4074	1.6×10^{-8}	4.4×10^{-10}	1.6×10^{-8}	0.0
47	$T_1 \to S_0$	$^7F_6 \to {}^5L_9$	0.0	−4195	1.6×10^{-9}	1.2×10^{-9}	3.3×10^{-10}	0.0
48	$T_1 \to S_0$	$^7F_6 \to {}^5G_3$	0.0	−4764	3.7×10^{-12}	2.1×10^{-12}	1.6×10^{-12}	0.0
49	$T_1 \to S_0$	$^7F_6 \to {}^5L_8$	0.0	−4977	1.1×10^{-11}	1.0×10^{-11}	5.9×10^{-13}	0.0
50	$T_1 \to S_0$	$^7F_6 \to {}^5L_7$	0.0	−5244	1.2×10^{-9}	1.3×10^{-12}	2.1×10^{-10}	9.8×10^{-10}
51	$T_1 \to S_0$	$^7F_6 \to {}^5L_6$	0.0	−5457	7.3×10^{-6}	0.0	0.0	7.3×10^{-6}
52	$T_1 \to S_0$	$^7F_6 \to {}^5H_7$	0.0	−7166	8.4×10^{-10}	0.0	0.0	8.4×10^{-10}
53	$T_1 \to S_0$	$^7F_6 \to {}^5H_6$	0.0	−8678	1.6×10^{-12}	0.0	0.0	1.6×10^{-12}
54	$T_1 \to S_0$	$^7F_6 \to {}^5H_5$	0.0	−9554	1.3×10^{-22}	0.0	0.0	1.3×10^{-22}
55	$T_1 \to S_0$	$^7F_6 \to {}^5F_5$	0.0	−10721	3.1×10^{-17}	0.0	0.0	3.1×10^{-17}
56	$T_1 \to S_0$	$^7F_6 \to {}^5I_7$	0.0	−12376	9.0×10^{-23}	0.0	0.0	9.0×10^{-23}
57	$T_1 \to S_0$	$^7F_6 \to {}^5I_6$	0.0	−13385	3.2×10^{-24}	0.0	0.0	3.2×10^{-24}
58	$T_1 \to S_0$	$^7F_6 \to {}^5I_5$	0.0	−13773	2.7×10^{-26}	0.0	0.0	2.7×10^{-26}
59	$T_1 \to S_0$	$^7F_6 \to {}^5K_5$	0.0	−17121	1.5×10^{-36}	0.0	0.0	1.5×10^{-36}
60	$T_1 \to S_0$	$^7F_6 \to {}^5K_7$	0.0	−17480	1.8×10^{-44}	0.0	0.0	1.8×10^{-44}
61	$T_1 \to S_0$	$^7F_5 \to {}^5D_4$	26.1	5817	1.1×10^{7}	8.4×10^{-2}	4.3×10^{2}	1.1×10^{7}
62	$T_1 \to S_0$	$^7F_5 \to {}^5D_3$	0.0	25	6.6×10^{1}	1.5×10^{-1}	6.6×10^{1}	0.0
63	$T_1 \to S_0$	$^7F_5 \to {}^5G_6$	73.6	−162	3.2×10^{7}	2.4×10^{-1}	2.4×10^{2}	3.2×10^{7}
64	$T_1 \to S_0$	$^7F_5 \to {}^5L_{10}$	0.0	−710	2.0×10^{-3}	2.0×10^{-3}	6.4×10^{-5}	0.0
65	$T_1 \to S_0$	$^7F_5 \to {}^5G_5$	0.3	−1506	1.5×10^{5}	1.7×10^{-4}	8.3×10^{-3}	1.5×10^{5}
66	$T_1 \to S_0$	$^7F_5 \to {}^5D_2$	0.0	−1846	8.7×10^{-5}	1.2×10^{-5}	7.6×10^{-5}	0.0
67	$T_1 \to S_0$	$^7F_5 \to {}^5G_4$	0.0	−2026	1.4×10^{3}	4.5×10^{-6}	3.1×10^{-3}	1.4×10^{3}
68	$T_1 \to S_0$	$^7F_5 \to {}^5L_9$	0.0	−2147	2.0×10^{-5}	1.5×10^{-5}	4.8×10^{-6}	0.0
69	$T_1 \to S_0$	$^7F_5 \to {}^5L_8$	0.0	−2929	7.0×10^{-7}	4.6×10^{-7}	2.4×10^{-7}	0.0
70	$T_1 \to S_0$	$^7F_5 \to {}^5L_7$	0.0	−3196	3.4×10^{-6}	3.6×10^{-8}	3.4×10^{-6}	0.0
71	$T_1 \to S_0$	$^7F_5 \to {}^5I_6$	0.0	−3409	5.0×10^{-2}	0.0	0.0	5.0×10^{-2}
72	$T_1 \to S_0$	$^7F_5 \to {}^5H_6$	0.0	−6630	1.9×10^{-8}	0.0	0.0	1.9×10^{-8}
73	$T_1 \to S_0$	$^7F_5 \to {}^5H_5$	0.0	−7506	2.0×10^{-9}	0.0	0.0	2.0×10^{-9}
74	$T_1 \to S_0$	$^7F_5 \to {}^5H_4$	0.0	−8078	2.0×10^{-10}	0.0	0.0	2.0×10^{-10}
75	$T_1 \to S_0$	$^7F_5 \to {}^5F_5$	0.0	−8673	4.2×10^{-12}	0.0	0.0	4.2×10^{-12}
76	$T_1 \to S_0$	$^7F_5 \to {}^5F_4$	0.0	−9113	1.1×10^{-12}	0.0	0.0	1.1×10^{-12}
77	$T_1 \to S_0$	$^7F_5 \to {}^5I_6$	0.0	−11337	1.0×10^{-19}	0.0	0.0	1.0×10^{-19}
78	$T_1 \to S_0$	$^7F_5 \to {}^5I_4$	0.0	−11347	9.6×10^{-23}	0.0	0.0	9.6×10^{-23}
79	$T_1 \to S_0$	$^7F_5 \to {}^5I_5$	0.0	−11725	7.2×10^{-22}	0.0	0.0	7.2×10^{-22}
80	$T_1 \to S_0$	$^7F_5 \to {}^5K_5$	0.0	−15073	4.0×10^{-31}	0.0	0.0	4.0×10^{-31}
				$\boldsymbol{W^T}$	3.2×10^{7}			
				$\boldsymbol{W^{T'}}$	1.1×10^{7}			

Supporting information

Table S6. Backward (Tb−to−ligand) IET rates for **[Tb(bpcd)(CoumA)(H_2O)]**.

p	donor	acceptor	contr. (%)	Δ (cm^{-1})	W_b (s^{-1})	W_{d-d} (s^{-1})	W_{d-m} (s^{-1})	W_{ex} (s^{-1})
1	$^5D_4 \to {}^7F_6$	$S_0 \to S_1$	0.0	−10043	4.9×10^{-17}	3.8×10^{-20}	4.9×10^{-17}	0.0
2	$^5D_3 \to {}^7F_6$	$S_0 \to S_1$	0.0	−4251	3.0×10^{-6}	1.7×10^{-6}	1.3×10^{-6}	0.0
3	$^5G_6 \to {}^7F_6$	$S_0 \to S_1$	0.0	−4064	2.0	1.9×10^{-4}	7.9×10^{-3}	2.0
4	$^5L_{10} \to {}^7F_6$	$S_0 \to S_1$	0.0	−3516	1.0×10^{-3}	9.4×10^{-4}	5.9×10^{-5}	0.0
5	$^5G_5 \to {}^7F_6$	$S_0 \to S_1$	0.0	−2720	1.6×10^{2}	2.6×10^{-2}	6.8	1.6×10^{2}
6	$^5G_4 \to {}^7F_6$	$S_0 \to S_1$	0.0	−2200	9.8	2.7×10^{-1}	9.5	0.0
7	$^5L_9 \to {}^7F_6$	$S_0 \to S_1$	0.0	−2079	1.5	1.2	3.3×10^{-1}	0.0
8	$^5G_3 \to {}^7F_6$	$S_0 \to S_1$	0.0	−1510	3.3	1.8	1.5	0.0
9	$^5L_8 \to {}^7F_6$	$S_0 \to S_1$	0.0	−1297	3.4×10^{1}	3.2×10^{1}	1.9	0.0
10	$^5L_7 \to {}^7F_6$	$S_0 \to S_1$	0.0	−1030	1.1×10^{4}	7.4×10^{1}	1.1×10^{4}	5.4
11	$^5L_6 \to {}^7F_6$	$S_0 \to S_1$	0.0	−817	4.1×10^{5}	0.0	0.0	4.1×10^{5}
12	$^5H_7 \to {}^7F_6$	$S_0 \to S_1$	0.6	892	2.0×10^{7}	0.0	0.0	2.0×10^{7}
13	$^5H_6 \to {}^7F_6$	$S_0 \to S_1$	4.5	2404	1.5×10^{8}	0.0	0.0	1.5×10^{8}
14	$^5H_5 \to {}^7F_6$	$S_0 \to S_1$	0.0	3280	1.6	0.0	0.0	1.6
15	$^5F_5 \to {}^7F_6$	$S_0 \to S_1$	6.0	4447	2.0×10^{8}	0.0	0.0	2.0×10^{8}
16	$^5I_7 \to {}^7F_6$	$S_0 \to S_1$	0.1	6102	3.1×10^{6}	0.0	0.0	3.1×10^{6}
17	$^5I_6 \to {}^7F_6$	$S_0 \to S_1$	0.9	7111	2.9×10^{7}	0.0	0.0	2.9×10^{7}
18	$^5I_5 \to {}^7F_6$	$S_0 \to S_1$	0.1	7499	2.2×10^{6}	0.0	0.0	2.2×10^{6}
19	$^5K_5 \to {}^7F_6$	$S_0 \to S_1$	0.0	10847	8.0×10^{3}	0.0	0.0	8.0×10^{3}
20	$^5K_7 \to {}^7F_6$	$S_0 \to S_1$	0.0	11206	4.9×10^{-4}	0.0	0.0	4.9×10^{-4}
21	$^5D_4 \to {}^7F_5$	$S_0 \to S_1$	0.0	−12091	2.0×10^{-20}	1.1×10^{-24}	5.5×10^{-21}	1.5×10^{-20}
22	$^5D_3 \to {}^7F_5$	$S_0 \to S_1$	0.0	−6299	3.5×10^{-8}	8.1×10^{-11}	3.5×10^{-8}	0.0
23	$^5G_6 \to {}^7F_5$	$S_0 \to S_1$	0.0	−6112	5.8×10^{-6}	4.1×10^{-10}	4.1×10^{-7}	5.4×10^{-6}
24	$^5L_{10} \to {}^7F_5$	$S_0 \to S_1$	0.0	−5564	5.7×10^{-10}	5.5×10^{-10}	1.8×10^{-11}	0.0
25	$^5G_5 \to {}^7F_5$	$S_0 \to S_1$	0.0	−4768	2.6×10^{-2}	3.1×10^{-7}	1.5×10^{-5}	2.6×10^{-2}
26	$^5D_2 \to {}^7F_5$	$S_0 \to S_1$	0.0	−4428	1.1×10^{-5}	1.5×10^{-6}	9.6×10^{-6}	0.0
27	$^5G_4 \to {}^7F_5$	$S_0 \to S_1$	0.0	−4248	6.3×10^{-2}	2.0×10^{-6}	1.4×10^{-3}	6.2×10^{-2}
28	$^5L_9 \to {}^7F_5$	$S_0 \to S_1$	0.0	−4127	1.4×10^{-5}	1.1×10^{-5}	3.5×10^{-6}	0.0
29	$^5L_8 \to {}^7F_5$	$S_0 \to S_1$	0.0	−3345	1.6×10^{-3}	1.1×10^{-3}	5.6×10^{-4}	0.0
30	$^5L_7 \to {}^7F_5$	$S_0 \to S_1$	0.0	−3078	1.4×10^{-1}	1.5×10^{-3}	1.4×10^{-1}	0.0
31	$^5I_6 \to {}^7F_5$	$S_0 \to S_1$	0.0	−2865	2.0	0.0	0.0	2.0
32	$^5H_6 \to {}^7F_5$	$S_0 \to S_1$	0.7	356	2.5×10^{7}	0.0	0.0	2.5×10^{7}
33	$^5H_5 \to {}^7F_5$	$S_0 \to S_1$	10.4	1232	3.5×10^{8}	0.0	0.0	3.5×10^{8}
34	$^5H_4 \to {}^7F_5$	$S_0 \to S_1$	26.8	1804	9.0×10^{8}	0.0	0.0	9.0×10^{8}
35	$^5F_5 \to {}^7F_5$	$S_0 \to S_1$	11.4	2399	3.8×10^{8}	0.0	0.0	3.8×10^{8}
36	$^5F_4 \to {}^7F_5$	$S_0 \to S_1$	38.1	2839	1.3×10^{9}	0.0	0.0	1.3×10^{9}
37	$^5I_6 \to {}^7F_5$	$S_0 \to S_1$	0.4	5063	1.3×10^{7}	0.0	0.0	1.3×10^{7}
38	$^5I_4 \to {}^7F_5$	$S_0 \to S_1$	0.0	5073	1.8×10^{4}	0.0	0.0	1.8×10^{4}
39	$^5I_5 \to {}^7F_5$	$S_0 \to S_1$	0.0	5451	8.6×10^{5}	0.0	0.0	8.6×10^{5}
40	$^5K_5 \to {}^7F_5$	$S_0 \to S_1$	0.0	8799	3.0×10^{4}	0.0	0.0	3.0×10^{4}
				W_b^S	3.4×10^{9}			
41	$^5D_4 \to {}^7F_6$	$S_0 \to T_1$	0.0	−3769	9.8×10^{-7}	7.6×10^{-10}	9.8×10^{-7}	0.0

42	$^5D_3 \rightarrow {}^7F_6$	$S_0 \rightarrow T_1$	0.0	2023	1.5×10^{-1}	8.3×10^{-2}	6.5×10^{-2}	0.0
43	$^5G_6 \rightarrow {}^7F_6$	$S_0 \rightarrow T_1$	48.7	2210	3.6×10^{8}	3.4	1.4×10^{2}	3.6×10^{8}
44	$^5L_{10} \rightarrow {}^7F_6$	$S_0 \rightarrow T_1$	0.0	2758	9.6×10^{-1}	9.0×10^{-1}	5.6×10^{-2}	0.0
45	$^5G_5 \rightarrow {}^7F_6$	$S_0 \rightarrow T_1$	2.8	3554	2.1×10^{7}	3.5×10^{-1}	9.1×10^{1}	2.1×10^{7}
46	$^5G_4 \rightarrow {}^7F_6$	$S_0 \rightarrow T_1$	0.0	4074	8.0	2.2×10^{-1}	7.8	0.0
47	$^5L_9 \rightarrow {}^7F_6$	$S_0 \rightarrow T_1$	0.0	4195	6.6×10^{-1}	5.2×10^{-1}	1.4×10^{-1}	0.0
48	$^5G_3 \rightarrow {}^7F_6$	$S_0 \rightarrow T_1$	0.0	4764	6.6×10^{-2}	3.7×10^{-2}	2.9×10^{-2}	0.0
49	$^5L_8 \rightarrow {}^7F_6$	$S_0 \rightarrow T_1$	0.0	4977	2.2×10^{-1}	2.1×10^{-1}	1.2×10^{-2}	0.0
50	$^5L_7 \rightarrow {}^7F_6$	$S_0 \rightarrow T_1$	0.0	5244	1.0×10^{2}	1.1×10^{-1}	1.7×10^{1}	8.3×10^{1}
51	$^5L_6 \rightarrow {}^7F_6$	$S_0 \rightarrow T_1$	0.3	5457	2.0×10^{6}	0.0	0.0	2.0×10^{6}
52	$^5H_7 \rightarrow {}^7F_6$	$S_0 \rightarrow T_1$	0.1	7166	7.5×10^{5}	0.0	0.0	7.5×10^{5}
53	$^5H_6 \rightarrow {}^7F_6$	$S_0 \rightarrow T_1$	0.3	8678	2.5×10^{6}	0.0	0.0	2.5×10^{6}
54	$^5H_5 \rightarrow {}^7F_6$	$S_0 \rightarrow T_1$	0.0	9554	1.6×10^{-2}	0.0	0.0	1.6×10^{-2}
55	$^5F_5 \rightarrow {}^7F_6$	$S_0 \rightarrow T_1$	0.1	10721	1.1×10^{6}	0.0	0.0	1.1×10^{6}
56	$^5I_7 \rightarrow {}^7F_6$	$S_0 \rightarrow T_1$	0.0	12376	6.7×10^{3}	0.0	0.0	6.7×10^{3}
57	$^5I_6 \rightarrow {}^7F_6$	$S_0 \rightarrow T_1$	0.0	13385	3.6×10^{4}	0.0	0.0	3.6×10^{4}
58	$^5I_5 \rightarrow {}^7F_6$	$S_0 \rightarrow T_1$	0.0	13773	2.3×10^{3}	0.0	0.0	2.3×10^{3}
59	$^5K_5 \rightarrow {}^7F_6$	$S_0 \rightarrow T_1$	0.0	17121	1.3	0.0	0.0	1.3
60	$^5K_7 \rightarrow {}^7F_6$	$S_0 \rightarrow T_1$	0.0	17480	6.8×10^{-8}	0.0	0.0	6.8×10^{-8}
61	$^5D_4 \rightarrow {}^7F_5$	$S_0 \rightarrow T_1$	0.0	−5817	8.9×10^{-6}	6.6×10^{-14}	3.4×10^{-10}	8.9×10^{-6}
62	$^5D_3 \rightarrow {}^7F_5$	$S_0 \rightarrow T_1$	0.0	−25	9.2×10^{1}	2.1×10^{-1}	9.2×10^{1}	0.0
63	$^5G_6 \rightarrow {}^7F_5$	$S_0 \rightarrow T_1$	7.9	162	5.9×10^{7}	4.5×10^{-1}	4.4×10^{2}	5.9×10^{7}
64	$^5L_{10} \rightarrow {}^7F_5$	$S_0 \rightarrow T_1$	0.0	710	3.3×10^{-2}	3.2×10^{-2}	1.0×10^{-3}	0.0
65	$^5G_5 \rightarrow {}^7F_5$	$S_0 \rightarrow T_1$	28.2	1506	2.1×10^{8}	2.5×10^{-1}	1.2×10^{1}	2.1×10^{8}
66	$^5D_2 \rightarrow {}^7F_5$	$S_0 \rightarrow T_1$	0.0	1846	1.4	1.9×10^{-1}	1.2	0.0
67	$^5G_4 \rightarrow {}^7F_5$	$S_0 \rightarrow T_1$	4.0	2026	3.0×10^{7}	9.7×10^{-2}	6.7×10^{1}	3.0×10^{7}
68	$^5L_9 \rightarrow {}^7F_5$	$S_0 \rightarrow T_1$	0.0	2147	3.6×10^{-1}	2.7×10^{-1}	8.8×10^{-2}	0.0
69	$^5L_8 \rightarrow {}^7F_5$	$S_0 \rightarrow T_1$	0.0	2929	6.2×10^{-1}	4.1×10^{-1}	2.2×10^{-1}	0.0
70	$^5L_7 \rightarrow {}^7F_5$	$S_0 \rightarrow T_1$	0.0	3196	1.2×10^{1}	1.3×10^{-1}	1.2×10^{1}	0.0
71	$^5L_6 \rightarrow {}^7F_5$	$S_0 \rightarrow T_1$	0.1	3409	5.9×10^{5}	0.0	0.0	5.9×10^{5}
72	$^5H_6 \rightarrow {}^7F_5$	$S_0 \rightarrow T_1$	0.2	6630	1.2×10^{6}	0.0	0.0	1.2×10^{6}
73	$^5H_5 \rightarrow {}^7F_5$	$S_0 \rightarrow T_1$	1.5	7506	1.1×10^{7}	0.0	0.0	1.1×10^{7}
74	$^5H_4 \rightarrow {}^7F_5$	$S_0 \rightarrow T_1$	2.8	8078	2.0×10^{7}	0.0	0.0	2.0×10^{7}
75	$^5F_5 \rightarrow {}^7F_5$	$S_0 \rightarrow T_1$	0.8	8673	6.3×10^{6}	0.0	0.0	6.3×10^{6}
76	$^5F_4 \rightarrow {}^7F_5$	$S_0 \rightarrow T_1$	2.2	9113	1.7×10^{7}	0.0	0.0	1.7×10^{7}
77	$^5I_6 \rightarrow {}^7F_5$	$S_0 \rightarrow T_1$	0.0	11337	4.9×10^{4}	0.0	0.0	4.9×10^{4}
78	$^5I_4 \rightarrow {}^7F_5$	$S_0 \rightarrow T_1$	0.0	11347	7.0×10^{1}	0.0	0.0	7.0×10^{1}
79	$^5I_5 \rightarrow {}^7F_5$	$S_0 \rightarrow T_1$	0.0	11725	2.7×10^{3}	0.0	0.0	2.7×10^{3}
80	$^5K_5 \rightarrow {}^7F_5$	$S_0 \rightarrow T_1$	0.0	15073	1.5×10^{1}	0.0	0.0	1.5×10^{1}
				W_b^T	7.4×10^{8}			
				$W_b^{T'}$	9.8×10^{-6}			

Supporting information

Table S7. Forward (ligand−to−Tb) IET rates for **[Tb(bpcd)(CoumB)(H$_2$O)]**.

p	donor	acceptor	contr. (%)	Δ (cm^{-1})	W (s^{-1})	W_{d-d} (s^{-1})	W_{d-m} (s^{-1})	W_{ex} (s^{-1})
1	$S_1 \to S_0$	$^7F_6 \to {}^5D_4$	0.0	9916	4.5×10^{4}	3.2×10^{1}	4.5×10^{4}	0.0
2	$S_1 \to S_0$	$^7F_6 \to {}^5D_3$	0.0	4124	1.5×10^{3}	7.5×10^{2}	7.5×10^{2}	0.0
3	$S_1 \to S_0$	$^7F_6 \to {}^5G_6$	59.7	3937	8.3×10^{8}	6.2×10^{4}	2.9×10^{6}	8.3×10^{8}
4	$S_1 \to S_0$	$^7F_6 \to {}^5L_{10}$	0.0	3389	3.9×10^{4}	3.6×10^{4}	2.9×10^{3}	0.0
5	$S_1 \to S_0$	$^7F_6 \to {}^5G_5$	6.2	2593	8.6×10^{7}	1.1×10^{4}	3.2×10^{6}	8.3×10^{7}
6	$S_1 \to S_0$	$^7F_6 \to {}^5G_4$	0.0	2073	3.0×10^{5}	7.6×10^{3}	2.9×10^{5}	0.0
7	$S_1 \to S_0$	$^7F_6 \to {}^5L_9$	0.0	1952	5.4×10^{4}	4.0×10^{4}	1.4×10^{4}	0.0
8	$S_1 \to S_0$	$^7F_6 \to {}^5G_3$	0.0	1383	2.9×10^{3}	1.4×10^{3}	1.4×10^{3}	0.0
9	$S_1 \to S_0$	$^7F_6 \to {}^5L_8$	0.0	1170	2.4×10^{4}	2.2×10^{4}	1.7×10^{3}	0.0
10	$S_1 \to S_0$	$^7F_6 \to {}^5L_7$	0.1	903	2.0×10^{6}	1.2×10^{4}	2.0×10^{6}	1.1×10^{3}
11	$S_1 \to S_0$	$^7F_6 \to {}^5L_6$	1.8	690	2.6×10^{7}	0.0	0.0	2.6×10^{7}
12	$S_1 \to S_0$	$^7F_6 \to {}^5H_7$	0.0	−1019	2.0×10^{5}	0.0	0.0	2.0×10^{5}
13	$S_1 \to S_0$	$^7F_6 \to {}^5H_6$	0.0	−2531	8.8×10^{2}	0.0	0.0	8.8×10^{2}
14	$S_1 \to S_0$	$^7F_6 \to {}^5H_5$	0.0	−3407	1.1×10^{-7}	0.0	0.0	1.1×10^{-7}
15	$S_1 \to S_0$	$^7F_6 \to {}^5F_5$	0.0	−4574	5.0×10^{-2}	0.0	0.0	5.0×10^{-2}
16	$S_1 \to S_0$	$^7F_6 \to {}^5I_7$	0.0	−6229	3.5×10^{-7}	0.0	0.0	3.5×10^{-7}
17	$S_1 \to S_0$	$^7F_6 \to {}^5I_6$	0.0	−7238	2.2×10^{-8}	0.0	0.0	2.2×10^{-8}
18	$S_1 \to S_0$	$^7F_6 \to {}^5I_5$	0.0	−7626	2.2×10^{-10}	0.0	0.0	2.2×10^{-10}
19	$S_1 \to S_0$	$^7F_6 \to {}^5K_5$	0.0	−10974	7.3×10^{-20}	0.0	0.0	7.3×10^{-20}
20	$S_1 \to S_0$	$^7F_6 \to {}^5K_7$	0.0	−11333	1.1×10^{-27}	0.0	0.0	1.1×10^{-27}
21	$S_1 \to S_0$	$^7F_5 \to {}^5D_4$	0.0	11964	4.8×10^{5}	2.2×10^{1}	1.2×10^{5}	3.6×10^{5}
22	$S_1 \to S_0$	$^7F_5 \to {}^5D_3$	0.0	6172	4.0×10^{5}	8.6×10^{2}	4.0×10^{5}	0.0
23	$S_1 \to S_0$	$^7F_5 \to {}^5G_6$	4.1	5985	5.7×10^{7}	3.3×10^{3}	3.5×10^{6}	5.3×10^{7}
24	$S_1 \to S_0$	$^7F_5 \to {}^5L_{10}$	0.0	5437	5.2×10^{2}	5.0×10^{2}	2.2×10^{1}	0.0
25	$S_1 \to S_0$	$^7F_5 \to {}^5G_5$	23.7	4641	3.3×10^{8}	3.2×10^{3}	1.6×10^{5}	3.3×10^{8}
26	$S_1 \to S_0$	$^7F_5 \to {}^5D_2$	0.0	4301	1.2×10^{4}	1.3×10^{3}	1.1×10^{4}	0.0
27	$S_1 \to S_0$	$^7F_5 \to {}^5G_4$	3.7	4121	5.2×10^{7}	1.3×10^{3}	9.9×10^{5}	5.1×10^{7}
28	$S_1 \to S_0$	$^7F_5 \to {}^5L_9$	0.0	4000	1.2×10^{4}	8.5×10^{3}	3.5×10^{3}	0.0
29	$S_1 \to S_0$	$^7F_5 \to {}^5L_8$	0.0	3218	2.9×10^{4}	1.7×10^{4}	1.1×10^{4}	0.0
30	$S_1 \to S_0$	$^7F_5 \to {}^5L_7$	0.0	2951	5.8×10^{5}	5.7×10^{3}	5.7×10^{5}	0.0
31	$S_1 \to S_0$	$^7F_5 \to {}^5I_6$	0.2	2738	3.0×10^{6}	0.0	0.0	3.0×10^{6}
32	$S_1 \to S_0$	$^7F_5 \to {}^5H_6$	0.2	−483	3.5×10^{6}	0.0	0.0	3.5×10^{6}
33	$S_1 \to S_0$	$^7F_5 \to {}^5H_5$	0.0	−1359	5.9×10^{5}	0.0	0.0	5.9×10^{5}
34	$S_1 \to S_0$	$^7F_5 \to {}^5H_4$	0.0	−1931	7.8×10^{4}	0.0	0.0	7.8×10^{4}
35	$S_1 \to S_0$	$^7F_5 \to {}^5F_5$	0.0	−2526	2.3×10^{3}	0.0	0.0	2.3×10^{3}
36	$S_1 \to S_0$	$^7F_5 \to {}^5F_4$	0.0	−2966	7.5×10^{2}	0.0	0.0	7.5×10^{2}
37	$S_1 \to S_0$	$^7F_5 \to {}^5I_6$	0.0	−5190	2.3×10^{-4}	0.0	0.0	2.3×10^{-4}
38	$S_1 \to S_0$	$^7F_5 \to {}^5I_4$	0.0	−5200	2.2×10^{-7}	0.0	0.0	2.2×10^{-7}
39	$S_1 \to S_0$	$^7F_5 \to {}^5I_5$	0.0	−5578	2.0×10^{-6}	0.0	0.0	2.0×10^{-6}
40	$S_1 \to S_0$	$^7F_5 \to {}^5K_5$	0.0	−8926	6.6×10^{-15}	0.0	0.0	6.6×10^{-15}
				W^S	1.4×10^{9}			
41	$T_1 \to S_0$	$^7F_6 \to {}^5D_4$	0.0	3479	5.6×10^{1}	4.2×10^{-2}	5.6×10^{1}	0.0

42	$T_1 \rightarrow S_0$	$^7F_6 \rightarrow {}^5D_3$	0.0	−2313	1.0×10^{-6}	5.4×10^{-7}	5.0×10^{-7}	0.0
43	$T_1 \rightarrow S_0$	$^7F_6 \rightarrow {}^5G_6$	0.0	−2500	2.1×10^{3}	1.7×10^{-5}	7.4×10^{-4}	2.1×10^{3}
44	$T_1 \rightarrow S_0$	$^7F_6 \rightarrow {}^5L_{10}$	0.0	−3048	5.4×10^{-7}	5.0×10^{-7}	3.7×10^{-8}	0.0
45	$T_1 \rightarrow S_0$	$^7F_6 \rightarrow {}^5G_5$	0.0	−3844	1.5×10^{-1}	2.2×10^{-9}	5.9×10^{-7}	1.5×10^{-1}
46	$T_1 \rightarrow S_0$	$^7F_6 \rightarrow {}^5G_4$	0.0	−4364	3.4×10^{-9}	8.8×10^{-11}	3.3×10^{-9}	0.0
47	$T_1 \rightarrow S_0$	$^7F_6 \rightarrow {}^5L_9$	0.0	−4485	3.2×10^{-10}	2.4×10^{-10}	7.7×10^{-11}	0.0
48	$T_1 \rightarrow S_0$	$^7F_6 \rightarrow {}^5G_3$	0.0	−5054	7.8×10^{-13}	4.1×10^{-13}	3.8×10^{-13}	0.0
49	$T_1 \rightarrow S_0$	$^7F_6 \rightarrow {}^5L_8$	0.0	−5267	2.1×10^{-12}	2.0×10^{-12}	1.4×10^{-13}	0.0
50	$T_1 \rightarrow S_0$	$^7F_6 \rightarrow {}^5L_7$	0.0	−5534	2.6×10^{-10}	2.6×10^{-13}	4.2×10^{-11}	2.2×10^{-10}
51	$T_1 \rightarrow S_0$	$^7F_6 \rightarrow {}^5L_6$	0.0	−5747	1.6×10^{-6}	0.0	0.0	1.6×10^{-6}
52	$T_1 \rightarrow S_0$	$^7F_6 \rightarrow {}^5H_7$	0.0	−7456	1.8×10^{-10}	0.0	0.0	1.8×10^{-10}
53	$T_1 \rightarrow S_0$	$^7F_6 \rightarrow {}^5H_6$	0.0	−8968	3.3×10^{-13}	0.0	0.0	3.3×10^{-13}
54	$T_1 \rightarrow S_0$	$^7F_6 \rightarrow {}^5H_5$	0.0	−9844	2.6×10^{-23}	0.0	0.0	2.6×10^{-23}
55	$T_1 \rightarrow S_0$	$^7F_6 \rightarrow {}^5F_5$	0.0	−11011	6.1×10^{-18}	0.0	0.0	6.1×10^{-18}
56	$T_1 \rightarrow S_0$	$^7F_6 \rightarrow {}^5I_7$	0.0	−12666	1.7×10^{-23}	0.0	0.0	1.7×10^{-23}
57	$T_1 \rightarrow S_0$	$^7F_6 \rightarrow {}^5I_6$	0.0	−13675	5.9×10^{-25}	0.0	0.0	5.9×10^{-25}
58	$T_1 \rightarrow S_0$	$^7F_6 \rightarrow {}^5I_5$	0.0	−14063	4.8×10^{-27}	0.0	0.0	4.8×10^{-27}
59	$T_1 \rightarrow S_0$	$^7F_6 \rightarrow {}^5K_5$	0.0	−17411	2.5×10^{-37}	0.0	0.0	2.5×10^{-37}
60	$T_1 \rightarrow S_0$	$^7F_6 \rightarrow {}^5K_7$	0.0	−17770	3.0×10^{-45}	0.0	0.0	3.0×10^{-45}
61	$T_1 \rightarrow S_0$	$^7F_5 \rightarrow {}^5D_4$	62.4	5527	1.4×10^{7}	9.1×10^{-2}	4.7×10^{2}	1.4×10^{7}
62	$T_1 \rightarrow S_0$	$^7F_5 \rightarrow {}^5D_3$	0.0	−265	1.7×10^{1}	3.8×10^{-2}	1.7×10^{1}	0.0
63	$T_1 \rightarrow S_0$	$^7F_5 \rightarrow {}^5G_6$	37.4	−452	8.1×10^{6}	5.4×10^{-2}	5.6×10^{1}	8.1×10^{6}
64	$T_1 \rightarrow S_0$	$^7F_5 \rightarrow {}^5L_{10}$	0.0	−1000	4.4×10^{-4}	4.3×10^{-4}	1.7×10^{-5}	0.0
65	$T_1 \rightarrow S_0$	$^7F_5 \rightarrow {}^5G_5$	0.2	−1796	3.6×10^{4}	3.7×10^{-5}	1.9×10^{-3}	3.6×10^{4}
66	$T_1 \rightarrow S_0$	$^7F_5 \rightarrow {}^5D_2$	0.0	−2136	2.1×10^{-5}	2.5×10^{-6}	1.9×10^{-5}	0.0
67	$T_1 \rightarrow S_0$	$^7F_5 \rightarrow {}^5G_4$	0.0	−2316	3.4×10^{2}	9.5×10^{-7}	6.9×10^{-4}	3.4×10^{2}
68	$T_1 \rightarrow S_0$	$^7F_5 \rightarrow {}^5L_9$	0.0	−2437	4.3×10^{-6}	3.2×10^{-6}	1.2×10^{-6}	0.0
69	$T_1 \rightarrow S_0$	$^7F_5 \rightarrow {}^5L_8$	0.0	−3219	1.5×10^{-7}	9.5×10^{-8}	5.8×10^{-8}	0.0
70	$T_1 \rightarrow S_0$	$^7F_5 \rightarrow {}^5L_7$	0.0	−3486	7.4×10^{-7}	7.5×10^{-9}	7.3×10^{-7}	0.0
71	$T_1 \rightarrow S_0$	$^7F_5 \rightarrow {}^5I_6$	0.0	−3699	1.2×10^{-2}	0.0	0.0	1.2×10^{-2}
72	$T_1 \rightarrow S_0$	$^7F_5 \rightarrow {}^5H_6$	0.0	−6920	4.1×10^{-9}	0.0	0.0	4.1×10^{-9}
73	$T_1 \rightarrow S_0$	$^7F_5 \rightarrow {}^5H_5$	0.0	−7796	4.3×10^{-10}	0.0	0.0	4.3×10^{-10}
74	$T_1 \rightarrow S_0$	$^7F_5 \rightarrow {}^5H_4$	0.0	−8368	4.1×10^{-11}	0.0	0.0	4.1×10^{-11}
75	$T_1 \rightarrow S_0$	$^7F_5 \rightarrow {}^5F_5$	0.0	−8963	8.7×10^{-13}	0.0	0.0	8.7×10^{-13}
76	$T_1 \rightarrow S_0$	$^7F_5 \rightarrow {}^5F_4$	0.0	−9403	2.2×10^{-13}	0.0	0.0	2.2×10^{-13}
77	$T_1 \rightarrow S_0$	$^7F_5 \rightarrow {}^5I_6$	0.0	−11627	1.9×10^{-20}	0.0	0.0	1.9×10^{-20}
78	$T_1 \rightarrow S_0$	$^7F_5 \rightarrow {}^5I_4$	0.0	−11637	1.8×10^{-23}	0.0	0.0	1.8×10^{-23}
79	$T_1 \rightarrow S_0$	$^7F_5 \rightarrow {}^5I_5$	0.0	−12015	1.4×10^{-22}	0.0	0.0	1.4×10^{-22}
80	$T_1 \rightarrow S_0$	$^7F_5 \rightarrow {}^5K_5$	0.0	−15363	7.0×10^{-22}	0.0	0.0	7.0×10^{-32}
				$\boldsymbol{W^T}$	8.2×10^{6}			
				$\boldsymbol{W^{T'}}$	1.4×10^{7}			

Table S8. Backward (Tb−to−ligand) IET rates for **[Tb(bpcd)(CoumB)(H_2O)]**.

p	donor	acceptor	contr. (%)	Δ (cm^{-1})	W_b (s^{-1})	W_{d-d} (s^{-1})	W_{d-m} (s^{-1})	W_{ex} (s^{-1})
1	$^5D_4\rightarrow^7F_6$	$S_0\rightarrow S_1$	0.0	−9916	1.1×10^{-16}	7.7×10^{-20}	1.1×10^{-16}	0.0
2	$^5D_3\rightarrow^7F_6$	$S_0\rightarrow S_1$	0.0	−4124	6.3×10^{-6}	3.2×10^{-6}	3.2×10^{-6}	0.0
3	$^5G_6\rightarrow^7F_6$	$S_0\rightarrow S_1$	0.0	−3937	4.7	3.5×10^{-4}	1.6×10^{-2}	4.6
4	$^5L_{10}\rightarrow^7F_6$	$S_0\rightarrow S_1$	0.0	−3389	1.9×10^{-3}	1.8×10^{-3}	1.4×10^{-4}	0.0
5	$^5G_5\rightarrow^7F_6$	$S_0\rightarrow S_1$	0.0	−2593	3.8×10^{2}	4.9×10^{-2}	1.4×10^{1}	3.6×10^{2}
6	$^5G_4\rightarrow^7F_6$	$S_0\rightarrow S_1$	0.0	−2073	2.0×10^{1}	4.9×10^{-1}	1.9×10^{1}	0.0
7	$^5L_9\rightarrow^7F_6$	$S_0\rightarrow S_1$	0.0	−1952	3.0	2.2	7.6×10^{-1}	0.0
8	$^5G_3\rightarrow^7F_6$	$S_0\rightarrow S_1$	0.0	−1383	6.7	3.4	3.4	0.0
9	$^5L_8\rightarrow^7F_6$	$S_0\rightarrow S_1$	0.0	−1170	6.4×10^{1}	5.9×10^{1}	4.5	0.0
10	$^5L_7\rightarrow^7F_6$	$S_0\rightarrow S_1$	0.0	−903	2.3×10^{4}	1.4×10^{2}	2.3×10^{4}	1.2×10^{1}
11	$^5L_6\rightarrow^7F_6$	$S_0\rightarrow S_1$	0.0	−690	9.2×10^{5}	0.0	0.0	9.2×10^{5}
12	$^5H_7\rightarrow^7F_6$	$S_0\rightarrow S_1$	0.6	1019	2.4×10^{7}	0.0	0.0	2.4×10^{7}
13	$^5H_6\rightarrow^7F_6$	$S_0\rightarrow S_1$	4.5	2531	1.8×10^{8}	0.0	0.0	1.8×10^{8}
14	$^5H_5\rightarrow^7F_6$	$S_0\rightarrow S_1$	0.0	3407	1.9	0.0	0.0	1.9
15	$^5F_5\rightarrow^7F_6$	$S_0\rightarrow S_1$	5.8	4574	2.3×10^{8}	0.0	0.0	2.3×10^{8}
16	$^5I_7\rightarrow^7F_6$	$S_0\rightarrow S_1$	0.1	6229	3.4×10^{6}	0.0	0.0	3.4×10^{6}
17	$^5I_6\rightarrow^7F_6$	$S_0\rightarrow S_1$	0.8	7238	3.2×10^{7}	0.0	0.0	3.2×10^{7}
18	$^5I_5\rightarrow^7F_6$	$S_0\rightarrow S_1$	0.1	7626	2.5×10^{6}	0.0	0.0	2.5×10^{6}
19	$^5K_5\rightarrow^7F_6$	$S_0\rightarrow S_1$	0.0	10974	8.6×10^{3}	0.0	0.0	8.6×10^{3}
20	$^5K_7\rightarrow^7F_6$	$S_0\rightarrow S_1$	0.0	11333	5.3×10^{-4}	0.0	0.0	5.3×10^{-4}
21	$^5D_4\rightarrow^7F_5$	$S_0\rightarrow S_1$	0.0	−11964	4.9×10^{-20}	2.3×10^{-24}	1.2×10^{-20}	3.7×10^{-20}
22	$^5D_3\rightarrow^7F_5$	$S_0\rightarrow S_1$	0.0	−6172	7.4×10^{-8}	1.6×10^{-10}	7.3×10^{-8}	0.0
23	$^5G_6\rightarrow^7F_5$	$S_0\rightarrow S_1$	0.0	−5985	1.4×10^{-5}	8.0×10^{-10}	8.5×10^{-7}	1.3×10^{-5}
24	$^5L_{10}\rightarrow^7F_5$	$S_0\rightarrow S_1$	0.0	−5437	1.1×10^{-9}	1.1×10^{-9}	4.7×10^{-11}	0.0
25	$^5G_5\rightarrow^7F_5$	$S_0\rightarrow S_1$	0.0	−4641	6.2×10^{-2}	5.9×10^{-7}	3.1×10^{-5}	6.2×10^{-2}
26	$^5D_2\rightarrow^7F_5$	$S_0\rightarrow S_1$	0.0	−4301	2.6×10^{-5}	2.8×10^{-6}	2.3×10^{-5}	0.0
27	$^5G_4\rightarrow^7F_5$	$S_0\rightarrow S_1$	0.0	−4121	1.5×10^{-1}	3.8×10^{-6}	2.8×10^{-3}	1.4×10^{-1}
28	$^5L_9\rightarrow^7F_5$	$S_0\rightarrow S_1$	0.0	−4000	2.9×10^{-5}	2.0×10^{-5}	8.3×10^{-6}	0.0
29	$^5L_8\rightarrow^7F_5$	$S_0\rightarrow S_1$	0.0	−3218	3.3×10^{-3}	2.0×10^{-3}	1.3×10^{-3}	0.0
30	$^5L_7\rightarrow^7F_5$	$S_0\rightarrow S_1$	0.0	−2951	2.8×10^{-1}	2.7×10^{-3}	2.7×10^{-1}	0.0
31	$^5I_6\rightarrow^7F_5$	$S_0\rightarrow S_1$	0.0	−2738	4.7	0.0	0.0	4.7
32	$^5H_6\rightarrow^7F_5$	$S_0\rightarrow S_1$	0.8	483	3.0×10^{7}	0.0	0.0	3.0×10^{7}
33	$^5H_5\rightarrow^7F_5$	$S_0\rightarrow S_1$	10.5	1359	4.1×10^{8}	0.0	0.0	4.1×10^{8}
34	$^5H_4\rightarrow^7F_5$	$S_0\rightarrow S_1$	27.0	1931	1.1×10^{9}	0.0	0.0	1.1×10^{9}
35	$^5F_5\rightarrow^7F_5$	$S_0\rightarrow S_1$	11.4	2526	4.5×10^{8}	0.0	0.0	4.5×10^{8}
36	$^5F_4\rightarrow^7F_5$	$S_0\rightarrow S_1$	38.0	2966	1.5×10^{9}	0.0	0.0	1.5×10^{9}
37	$^5I_6\rightarrow^7F_5$	$S_0\rightarrow S_1$	0.4	5190	1.4×10^{7}	0.0	0.0	1.4×10^{7}
38	$^5I_4\rightarrow^7F_5$	$S_0\rightarrow S_1$	0.0	5200	2.1×10^{4}	0.0	0.0	2.1×10^{4}
39	$^5I_5\rightarrow^7F_5$	$S_0\rightarrow S_1$	0.0	5578	9.8×10^{5}	0.0	0.0	9.8×10^{5}
40	$^5K_5\rightarrow^7F_5$	$S_0\rightarrow S_1$	0.0	8926	3.3×10^{4}	0.0	0.0	3.3×10^{4}
				W_b^S	3.9×10^{9}			
41	$^5D_4\rightarrow^7F_6$	$S_0\rightarrow T_1$	0.0	−3479	4.2×10^{-6}	3.1×10^{-9}	4.2×10^{-6}	0.0

42	$^5D_3\rightarrow^7F_6$	$S_0\rightarrow T_1$	0.0	2313	1.4×10^{-1}	7.1×10^{-2}	6.5×10^{-2}	0.0
43	$^5G_6\rightarrow^7F_6$	$S_0\rightarrow T_1$	48.8	2500	3.6×10^{8}	2.9	1.3×10^{2}	3.6×10^{8}
44	$^5L_{10}\rightarrow^7F_6$	$S_0\rightarrow T_1$	0.0	3048	8.1×10^{-1}	7.6×10^{-1}	5.6×10^{-2}	0.0
45	$^5G_5\rightarrow^7F_6$	$S_0\rightarrow T_1$	2.7	3844	2.0×10^{7}	2.9×10^{-1}	7.9×10^{1}	2.0×10^{7}
46	$^5G_4\rightarrow^7F_6$	$S_0\rightarrow T_1$	0.0	4364	6.9	1.8×10^{-1}	6.7	0.0
47	$^5L_9\rightarrow^7F_6$	$S_0\rightarrow T_1$	0.0	4485	5.5×10^{-1}	4.2×10^{-1}	1.3×10^{-1}	0.0
48	$^5G_3\rightarrow^7F_6$	$S_0\rightarrow T_1$	0.0	5054	5.7×10^{-2}	3.0×10^{-2}	2.7×10^{-2}	0.0
49	$^5L_8\rightarrow^7F_6$	$S_0\rightarrow T_1$	0.0	5267	1.8×10^{-1}	1.6×10^{-1}	1.1×10^{-2}	0.0
50	$^5L_7\rightarrow^7F_6$	$S_0\rightarrow T_1$	0.0	5534	9.0×10^{1}	9.0×10^{-2}	1.5×10^{1}	7.6×10^{1}
51	$^5L_6\rightarrow^7F_6$	$S_0\rightarrow T_1$	0.2	5747	1.8×10^{6}	0.0	0.0	1.8×10^{6}
52	$^5H_7\rightarrow^7F_6$	$S_0\rightarrow T_1$	0.1	7456	6.6×10^{5}	0.0	0.0	6.6×10^{5}
53	$^5H_6\rightarrow^7F_6$	$S_0\rightarrow T_1$	0.3	8968	2.1×10^{6}	0.0	0.0	2.1×10^{6}
54	$^5H_5\rightarrow^7F_6$	$S_0\rightarrow T_1$	0.0	9844	1.3×10^{-2}	0.0	0.0	1.3×10^{-2}
55	$^5F_5\rightarrow^7F_6$	$S_0\rightarrow T_1$	0.1	11011	8.6×10^{5}	0.0	0.0	8.6×10^{5}
56	$^5I_7\rightarrow^7F_6$	$S_0\rightarrow T_1$	0.0	12666	5.1×10^{3}	0.0	0.0	5.1×10^{3}
57	$^5I_6\rightarrow^7F_6$	$S_0\rightarrow T_1$	0.0	13675	2.7×10^{4}	0.0	0.0	2.7×10^{4}
58	$^5I_5\rightarrow^7F_6$	$S_0\rightarrow T_1$	0.0	14063	1.7×10^{3}	0.0	0.0	1.7×10^{3}
59	$^5K_5\rightarrow^7F_6$	$S_0\rightarrow T_1$	0.0	17411	9.1×10^{-1}	0.0	0.0	9.1×10^{-1}
60	$^5K_7\rightarrow^7F_6$	$S_0\rightarrow T_1$	0.0	17770	4.5×10^{-8}	0.0	0.0	4.5×10^{-8}
61	$^5D_4\rightarrow^7F_5$	$S_0\rightarrow T_1$	0.0	−5527	4.3×10^{-5}	2.9×10^{-13}	1.5×10^{-9}	4.3×10^{-5}
62	$^5D_3\rightarrow^7F_5$	$S_0\rightarrow T_1$	0.0	265	9.9×10^{1}	2.2×10^{-1}	9.9×10^{1}	0.0
63	$^5G_6\rightarrow^7F_5$	$S_0\rightarrow T_1$	8.3	452	6.1×10^{7}	4.0×10^{-1}	4.2×10^{2}	6.1×10^{7}
64	$^5L_{10}\rightarrow^7F_5$	$S_0\rightarrow T_1$	0.0	1000	2.9×10^{-2}	2.8×10^{-2}	1.1×10^{-3}	0.0
65	$^5G_5\rightarrow^7F_5$	$S_0\rightarrow T_1$	28.8	1796	2.1×10^{8}	2.2×10^{-1}	1.1×10^{1}	2.1×10^{8}
66	$^5D_2\rightarrow^7F_5$	$S_0\rightarrow T_1$	0.0	2136	1.4	1.6×10^{-1}	1.2	0.0
67	$^5G_4\rightarrow^7F_5$	$S_0\rightarrow T_1$	4.1	2316	3.0×10^{7}	8.3×10^{-2}	6.0×10^{1}	3.0×10^{7}
68	$^5L_9\rightarrow^7F_5$	$S_0\rightarrow T_1$	0.0	2437	3.2×10^{-1}	2.3×10^{-1}	8.8×10^{-2}	0.0
69	$^5L_8\rightarrow^7F_5$	$S_0\rightarrow T_1$	0.0	3219	5.5×10^{-1}	3.4×10^{-1}	2.1×10^{-1}	0.0
70	$^5L_7\rightarrow^7F_5$	$S_0\rightarrow T_1$	0.0	3486	1.1×10^{1}	1.1×10^{-1}	1.1×10^{1}	0.0
71	$^5L_6\rightarrow^7F_5$	$S_0\rightarrow T_1$	0.1	3699	5.7×10^{5}	0.0	0.0	5.7×10^{5}
72	$^5H_6\rightarrow^7F_5$	$S_0\rightarrow T_1$	0.2	6920	1.1×10^{6}	0.0	0.0	1.1×10^{6}
73	$^5H_5\rightarrow^7F_5$	$S_0\rightarrow T_1$	1.3	7796	9.3×10^{6}	0.0	0.0	9.3×10^{6}
74	$^5H_4\rightarrow^7F_5$	$S_0\rightarrow T_1$	2.4	8368	1.7×10^{7}	0.0	0.0	1.7×10^{7}
75	$^5F_5\rightarrow^7F_5$	$S_0\rightarrow T_1$	0.7	8963	5.3×10^{6}	0.0	0.0	5.3×10^{6}
76	$^5F_4\rightarrow^7F_5$	$S_0\rightarrow T_1$	1.9	9403	1.4×10^{7}	0.0	0.0	1.4×10^{7}
77	$^5I_6\rightarrow^7F_5$	$S_0\rightarrow T_1$	0.0	11627	3.8×10^{4}	0.0	0.0	3.8×10^{4}
78	$^5I_4\rightarrow^7F_5$	$S_0\rightarrow T_1$	0.0	11637	5.5×10^{1}	0.0	0.0	5.5×10^{1}
79	$^5I_5\rightarrow^7F_5$	$S_0\rightarrow T_1$	0.0	12015	2.1×10^{3}	0.0	0.0	2.1×10^{3}
80	$^5K_5\rightarrow^7F_5$	$S_0\rightarrow T_1$	0.0	15363	1.1×10^{1}	0.0	0.0	1.1×10^{1}
				W_b^T	7.3×10^{8}			
				$W_b^{T'}$	4.7×10^{-5}			

Supporting information

3.2. Multiphonon decay rates

The multiphonon decay rate W_{mp} (in s^{-1}) between adjacent excited states of the Ln(III) ion can be calculated from the energy gap law:

$$W_{mp} = W_0 e^{-(\alpha \cdot \Delta E)} \quad \text{(S8)}$$

where W_0 ($\approx 10^7$ s^{-1}) is the decay rate extrapolated to zero energy gap ($\Delta E \approx 0$) and α is a constant (in cm) that depends on the material.[17,18] Thus, for more energy spaced subsequently levels, the W_{mp} tends to decay drastically. According to Miyakawa and Dexter,[19] the α factor can be estimated by:

$$\alpha = \frac{1}{\hbar\varpi}\left|\ln\left(\frac{N}{S(n+1)}\right) - 1\right| \quad \text{(S9)}$$

where N ($= \Delta E/\hbar\varpi$) is the number of phonons created in the relaxation process and n is the phonon occupancy number following a Bose-Einstein distribution $n = 1/(\exp(\hbar\varpi/k_B T) - 1)$, where k_B is the Boltzmann constant and T the temperature. S is the Huang-Rhys factor which typical values are in the range of 0.02 to 0.10 for Ln(III) ions.[20–22] Considering the mean phonon energy ($\hbar\varpi$) attributed mainly to the C=O stretching mode (around 1700 cm^{-1}) and $S = 0.05$, the values of α is in the order of 10^{-3} and 10^{-4} cm, leading to multiphonon rates between adjacent levels of Eu(III) and Tb(III) between 10^6 and 10^7 s^{-1} (Table S9), as considered in our calculations.

Table S9. Values of the multiphonon decay rates (W_{mp}) for some of Eu(III) and Tb(III) excited states. The ΔE is the energy difference between adjacent levels. The parameter α was estimated using $S = 0.05$, $\hbar\varpi = 1700$ cm^{-1}, and $n = 0.288 \times 10^{-3}$.

Eu(III)	**ΔE (cm^{-1})**	**α ($\times 10^{-3}$ cm)**	**W_{mp} ($\times 10^6$ s^{-1})**	**Tb(III)**	**ΔE (cm^{-1})**	**α ($\times 10^{-3}$ cm)**	**W_{mp} ($\times 10^6$ s^{-1})**
$^5D_2 \rightarrow ^5D_1$	2456	1.390	0.329	$^5G_6 \rightarrow ^5D_3$	187	0.125	9.770
$^5D_3 \rightarrow ^5D_2$	2872	1.482	0.142	$^5L_{10} \rightarrow ^5G_6$	548	0.508	7.571
$^5L_6 \rightarrow ^5D_3$	970	0.844	4.411	$^5G_5 \rightarrow ^5L_{10}$	796	0.727	5.604
$^5L_7 \rightarrow ^5L_6$	1032	0.880	4.032	$^5D_2 \rightarrow ^5G_5$	340	0.227	9.257
$^5G_2 \rightarrow ^5L_7$	35	1.110	9.619	$^5G_4 \rightarrow ^5D_2$	180	0.147	9.739
$^5G_3 \rightarrow ^5G_2$	143	0.282	9.604	$^5L_9 \rightarrow ^5G_4$	121	0.381	9.550
$^5G_4 \rightarrow ^5G_3$	85	0.588	9.512	$^5G_3 \rightarrow ^5L_9$	569	0.530	7.397
$^5G_5 \rightarrow ^5G_4$	113	0.421	9.536	$^5L_8 \rightarrow ^5G_3$	213	0.048	9.898
$^5G_6 \rightarrow ^5G_5$	19	1.470	9.725	$^5L_7 \rightarrow ^5L_8$	267	0.085	9.776
$^5L_8 \rightarrow ^5G_6$	492	0.444	8.036	$^5G_2 \rightarrow ^5L_7$	74	0.670	9.516
$^5D_4 \rightarrow ^5L_8$	342	0.231	9.242	$^5L_6 \rightarrow ^5G_2$	79	0.631	9.513
$^5L_9 \rightarrow ^5D_4$	374	0.283	8.995	$^5D_1 \rightarrow ^5L_6$	1000	0.862	4.225
$^5L_{10} \rightarrow ^5L_9$	467	0.414	8.243	$^5D_0 \rightarrow ^5D_1$	614	0.575	7.027
$^5H_3 \rightarrow ^5L_{10}$	2436	1.385	0.342	$^5H_7 \rightarrow ^5D_0$	155	0.235	9.642
$^5H_4 \rightarrow ^5H_3$	282	0.117	9.675	$^5H_6 \rightarrow ^5H_7$	1512	1.105	1.881
$^5H_5 \rightarrow ^5H_4$	136	0.312	9.585	$^5H_5 \rightarrow ^5H_6$	876	0.784	5.033
$^5H_6 \rightarrow ^5H_5$	231	0.000	9.999	$^5H_4 \rightarrow ^5H_5$	572	0.533	7.372
$^5H_7 \rightarrow ^5H_6$	27	1.263	9.665	$^5F_5 \rightarrow ^5H_4$	595	0.556	7.182
		Average	**7.261**			**Average**	**7.775**

Supporting information

3.3. Rate equations model and quantum yield

The population dynamics for Eu(III) and Tb(III) Coumarin-based compounds can be described by an appropriate system of rate equations for the level normalized populations, set up based on the schematic energy level diagram shown in Figure 5, including forward and backward IET rates.

To simplify the setup of the rate equations, the populations of the levels (or groups of levels) are represented by η_N (where N ranges from 0 to 4). Specifically, η_0, η_1, η_2, η_3, and η_4 represent the populations of the ground state, T_1, S_1, levels above the emitting Eu(III) $^5D_0$ and Tb(III) $^5D_4$, and the Eu(III) $^5D_0$ and Tb(III) $^5D_4$, respectively. Thus, based on the IET rates and the schematic energy level diagram, a 5-level rate equation is given by:

$$\frac{d}{dt}\eta_0(t) = -\phi \cdot \eta_0(t) + \frac{1}{\tau_T}\eta_1(t) + \frac{1}{\tau_S}\eta_2(t) + \frac{1}{\tau_{Ln}}\eta_4(t) \tag{S10}$$

$$\frac{d}{dt}\eta_1(t) = -\left(\frac{1}{\tau_T} + W^T + W^T(^5D_J)\right)\eta_1(t) + W_{ISC} \cdot \eta_2(t) + W_b^T \cdot \eta_3(t) + W_b^T(^5D_J) \cdot \eta_4(t) \tag{S11}$$

$$\frac{d}{dt}\eta_2(t) = -\left(\frac{1}{\tau_S} + W_{ISC} + W^S\right)\eta_2(t) + \phi \cdot \eta_0(t) + W_b^S \cdot \eta_3(t) \tag{S12}$$

$$\frac{d}{dt}\eta_3(t) = -(W_{mp} + W_b^T + W_b^S)\eta_3(t) + W^S \cdot \eta_2(t) + W^T \cdot \eta_1(t) \tag{S13}$$

$$\frac{d}{dt}\eta_4(t) = -\left(\frac{1}{\tau_{Ln}} + W_b^T(^5D_J)\right)\eta_4(t) + W_{mp} \cdot \eta_3(t) + W^T(^5D_J) \cdot \eta_1(t) \tag{S14}$$

where τ_T, τ_S, and τ_{Ln} (τ_{obs} in Table 2) are the lifetimes of the T_1, S_1, and emitting levels ($^5D_0$ and $^5D_4$), respectively. W_{ISC} is the intersystem crossing rate $S_1 \rightarrow T_1$. W_{mp} is the average nonradiative energy decay between adjacent levels above the emitting ones, that is in the order of ~7×10^6 s^{-1} for Ln(III) chelates, as estimated in Table S9.[8] ϕ is the $S_0 \rightarrow S_1$ pumping rate.[23]

Numerically solving systems of differential equations involves a variety of methods, such as the 4th order Runge-Kutta method with fixed or adaptive step sizes, Adams-Bashford, and others [24]. In the present study, the Radau method [25] was employed due to its computational efficiency and its reliability in the context of lanthanide-based materials [26–32]. For these numerical simulations, it is essential to establish the initial conditions of the populations when time (t) equals zero. The initial population of the ground state is set to $\eta_0(0) = 1$ (Eq. S10), signifying that the system starts in its ground state, while the populations of other excited states η_n (with $n \neq 0$, Eqs. S11–S14) start with $\eta_n(0) = 0$.

To check if the set of differential equations (Eqs. S10–S14) are coupled and the model is consistent, the following condition must be satisfied:[26,33]

$$\frac{1}{t_f}\int_{t=0}^{t_f}\sum_n \eta_n(t)\,dt = 1 \qquad \text{for } t \neq 0 \tag{S15}$$

This relation ensures that population is conserved over time in the rate equation model.

The overall quantum yield, by its definition, is the ratio between emitted and absorbed photons, which can be represented by:[23]

$$\Phi_{ovl} = \frac{A_{rad}\cdot\eta_4}{\phi\cdot\eta_0} \tag{S16}$$

where A_{rad} is the radiative rate from the emitting level ($1/\tau_{rad}$, Table 2) and ϕ is the $S_0 \rightarrow S_1$ pumping rate. η_4 and η_0 is the population of the emitting and ground levels at the steady-state regime, respectively. In the simulations, A_{rad} was considered 450 s^{-1} for Tb(III) compounds, which is within the limit $A_{rad} < 1/\tau_{obs}$. As concluded elsewhere [23], the quantum yield is independent of the value of ϕ because the ratio $\eta_4/(\phi\cdot\eta_0)$ remains constant.

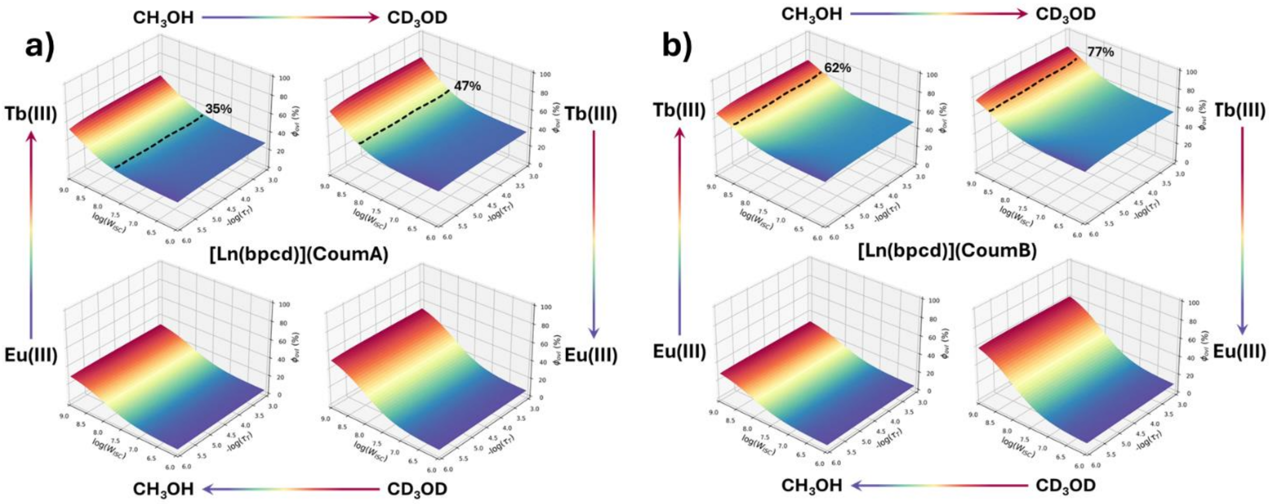

Figure S15. ϕ_{ovl} as a function of the W_{ISC} and τ_T for [Ln(bpcd)(CoumA)] (a) and for [Ln(bpcd)(CoumB)] (b). In these simulations, the τ_S was fixed at 10 ns.

3.4. Computational code

Below is an example of an input file (e.g. TbCoumA_CH3OH.txt) with some parameters previously calculated as IET rates that appear in the rate equation model:

```
# Example of an input file for the simulation of quantum yield (QY)
# The number of steps indicates the division of the range for W_ISC and τ_S

Arad = 450              # Radiative decay rate (1/τ_rad)
tau = 2.07e-3           # Observed lifetime (τ_obs)
tauT = 1e-5             # Triplet state lifetime (τ_T)
W_T = 3.2e7             # IET rate from triplet (W_T)
```

Supporting information

```
W_bT = 7.4e8            # Backward IET from Ln(III) to the triplet (W_bT)
W_T2 = 1.1e7            # IET from triplet state to the emitting level (W_T2)
W_bT2 = 9.8e-6          # Backward IET from the emitting level to the triplet state (W_bT2)
W_S = 1.11e9            # IET rate from singlet (W_S)
W_bS = 3.36e9           # Backward IET from Ln(III) to the singlet (W_bS)

W_ISC_start = 1e6       # Starting value for ISC rate
W_ISC_end = 1e9         # Ending value for ISC rate
tauS_start = 1e-6       # Starting value for singlet lifetime (τ_S)
tauS_end = 1e-9         # Ending value for singlet lifetime (τ_S)

steps = 100             # Number of steps for each variation (W_ISC and tauS) in the simulation
                        # the total number of calculations is given by steps²
```

The Python code below will extract the information from the input data and calculate the overall quantum yield (ϕ_{ovl}). To use the code, run:

```
python3 QYCalc.py <input.txt> <output.log> [<image.jpg>]
```

The generation of the image is optional.

```python
import sys
import os
import numpy as np
from scipy.integrate import solve_ivp
import matplotlib.pyplot as plt
from mpl_toolkits.mplot3d import Axes3D
import math
from tqdm import tqdm

print("╔═════════════════════════════════════════════════════════╗")
print("║             QYCalc V1.1 program (October 17, 2024)      ║")
print("╠═════════════════════════════════════════════════════════╣")
print("║     Albano N. Carneiro Neto      albanoneto@ua.pt       ║")
print("║                                                         ║")
print("║   Phantom-g, CICECO-Aveiro Institute of Materials       ║")
print("║   Department of Physics, University of Aveiro, Portugal ║")
print("╚═════════════════════════════════════════════════════════╝")

print("Reading the input data...\n")
def read_input_data(filename):
    input_data = {}

    # Check if the input file exists
    if not os.path.exists(filename):
        print(f"Error: File '{filename}' does not exist.")
        print("End of the program.")
        sys.exit(1)

    try:
        with open(filename, 'r') as file:
            for line in file:
                line = line.strip()
                if line.startswith("#") or not line:
                    continue
                if '=' in line:
                    key, value = line.split('=', 1)
                    value = value.split()[0]
                    input_data[key.strip()] = float(value)
    except IOError:
        print(f"Error: Could not read file '{filename}'.")
        sys.exit(1)

    # Check if required keys are given (e.g. Arad, phi, etc.)
    required_keys = ['Arad', 'tau', 'tauT', 'W_T', 'W_bT', 'W_T2', 'W_bT2', 'W_S', 'W_bS', 'steps']

    for key in required_keys:
        if key not in input_data:
            print(f"Error: Missing required input parameter '{key}' in the input file.")
            print("Please, insert the value of this parameter and run the code again...")
```

```
            print("End of the program.")
            sys.exit(1)

    return input_data

if len(sys.argv) < 3:
    print("Usage: python3 QYCalc.py <input_file> <output_file> [<output_image>]")
    print("You should provide at least the input and output file...")
    print("End of the program.")
    sys.exit(1)

input_file = sys.argv[1]
output_file = sys.argv[2]

# get output_image
output_image = sys.argv[3] if len(sys.argv) > 3 else None

# Reading the parameters
input_data = read_input_data(input_file)
phi = 200  # pumping rate
W_34 = 1e6 # average multiphonon decay between adjacent Ln(III) levels
Arad = input_data['Arad']
tau = input_data['tau']
tauT = input_data['tauT']
W_T = input_data['W_T']
W_bT = input_data['W_bT']
W_T2 = input_data['W_T2']
W_bT2 = input_data['W_bT2']
W_S = input_data['W_S']
W_bS = input_data['W_bS']
W_ISC_start = input_data['W_ISC_start']
W_ISC_end = input_data['W_ISC_end']
tauS_start = input_data['tauS_start']
tauS_end = input_data['tauS_end']
steps = int(input_data['steps'])

if Arad > 1 / tau:
    print(f"Error: Arad ({Arad} s-1) cannot be higher than 1/tau ({1/tau} s-1).")
    print("End of the program.")
    sys.exit(1)

print("The input file is ok.")
print("Running the calculation...")

# Rate equations model (5-levels)
def system_of_odes(t, y, phi, tau, tauT, tauS, W_34, W_T, W_bT, W_T2, W_bT2, W_S, W_bS, W_ISC):
    dydt = np.zeros(5)
    dydt[0] = -phi * y[0] + y[1] / tauT + y[2] / tauS + y[4] / tau
    dydt[1] = -(1/tauT + W_T + W_T2) * y[1] + W_ISC * y[2] + W_bT * y[3] + W_bT2 * y[4]
    dydt[2] = -(1/tauS + W_ISC + W_S) * y[2] + phi * y[0] + W_bS * y[3]
    dydt[3] = -(W_34 + W_bT + W_bS) * y[3] + W_S * y[2] + W_T * y[1]
    dydt[4] = -(1/tau + W_bT2) * y[4] + W_34 * y[3] + W_T2 * y[1]
    return dydt

# Initial conditions of the system ( t = 0)
y0 = [1, 0, 0, 0, 0]

# Time span for the solution
t_span = (0, 0.10)
t_eval = np.linspace(t_span[0], t_span[1], 2000)

# Step calculations for parameters
W_ISC_step = (W_ISC_end / W_ISC_start)**(1 / (steps - 1))
tauS_step = (tauS_end / tauS_start)**(1 / (steps - 1))

QY_values = []
log_W_ISC_values = []
minus_log_tauS_values = []

with open(output_file, "w") as output_file:
    output_file.write("╔═════════════════════════════════════════════════════════╗\n")
    output_file.write("║            QYCalc V1.1 program (October 17, 2024)       ║\n")
    output_file.write("╠═════════════════════════════════════════════════════════╣\n")
    output_file.write("║     Albano N. Carneiro Neto      albanoneto@ua.pt       ║\n")
    output_file.write("║                                                         ║\n")
    output_file.write("║   Phantom-g, CICECO-Aveiro Institute of Materials       ║\n")
    output_file.write("║   Department of Physics, University of Aveiro, Portugal ║\n")
    output_file.write("╚═════════════════════════════════════════════════════════╝\n")
    output_file.write("Quantum Yield (QY) calculations\n")
    output_file.write(f"Arad: {Arad}, phi: {phi}, tau: {tau}, tauT: {tauT}\n")
```

```
    output_file.write(f"W_ISC range: {W_ISC_start} to {W_ISC_end}, tauS range: {tauS_start} to {tauS_end}\n\n")
    output_file.write("╔════════════════════════════════╗\n")
    output_file.write("║   QY (%)  W_ISC (s-1)  tauS (s) ║\n")
    output_file.write("╠════════════════════════════════╣\n")

    total_iterations = steps * steps
    progress_bar = tqdm(total=total_iterations, desc="Calculation Progress", unit="step")

    W_ISC = W_ISC_start
    i = 0
    while i < steps:
        j = 0
        tauS = tauS_start
        while j < steps:
            # Solve the ODE system
            solution = solve_ivp(system_of_odes, t_span, y0, args=(phi, tau, tauT, tauS, W_34, W_T, W_bT, W_T2,
W_bT2, W_S, W_bS, W_ISC), t_eval=t_eval, method='Radau')

            y0_final = solution.y[0, -1]
            y4_final = solution.y[4, -1]

            # Calculate QY, log(W_ISC), and -log(tauS)
            QY = 100 * Arad * y4_final / (y0_final * phi)
            log_W_ISC = math.log10(W_ISC)
            minus_log_tauS = -math.log10(tauS)
            QY_values.append(QY)
            log_W_ISC_values.append(log_W_ISC)
            minus_log_tauS_values.append(minus_log_tauS)
            output_file.write(f"║ {QY:6.1f}  {W_ISC:10.2e}  {tauS:10.2e} ║\n")
            tauS *= tauS_step
            j += 1
            progress_bar.update(1)

        W_ISC *= W_ISC_step
        i += 1
    output_file.write("╚════════════════════════════════╝\n")
    output_file.write("End of program!\n")

progress_bar.close()

output_file.close()

if output_image:
    QY_values = np.array(QY_values)
    log_W_ISC_values = np.array(log_W_ISC_values)
    minus_log_tauS_values = np.array(minus_log_tauS_values)

    QY_values = QY_values.reshape((steps, steps))
    log_W_ISC_values = log_W_ISC_values.reshape((steps, steps))
    minus_log_tauS_values = minus_log_tauS_values.reshape((steps, steps))

    x_min = np.min(log_W_ISC_values)
    x_max = np.max(log_W_ISC_values)
    y_min = np.min(minus_log_tauS_values)
    y_max = np.max(minus_log_tauS_values)

    # Creating a 3D surface plot (if requested)
    fig = plt.figure(figsize=(10, 7), dpi=600)
    ax = fig.add_subplot(111, projection='3d')
    surf = ax.plot_surface(log_W_ISC_values, minus_log_tauS_values, QY_values, cmap='Spectral_r')

    ax.set_xlabel(r'log($W_{ISC}$)', fontsize=14)
    ax.set_ylabel(r'-log($\tau_{S}$)', fontsize=14)
    ax.set_zlabel(r'$\phi_{ovl}$ (%)', fontsize=14, rotation=90)

    ax.set_xlim(x_min, x_max)
    ax.set_ylim(y_min, y_max)
    ax.set_zlim(0, 100)

    ax.view_init(elev=30, azim=130)
    plt.savefig(output_image, format='jpg', dpi=600)
    plt.show()
```

4. References

Supporting information

(1) Stefanou, V.; Matiadis, D.; Melagraki, G.; Afantitis, A.; Athanasellis, G.; Igglessi-Markopoulou, O.; McKee, V.; Markopoulos, J. Functionalized 4-Hydroxy Coumarins: Novel Synthesis, Crystal Structure and DFT Calculations. *Molecules* **2011**, *16* (1), 384–402. https://doi.org/10.3390/molecules16010384.

(2) Athanasellis, G.; Melagraki, G.; Chatzidakis, H.; Afantitis, A.; Detsi, A.; Igglessi-Markopoulou, O.; Markopoulos, J. Novel Short-Step Synthesis of Functionalized γ-Phenyl-β-Hydroxybutenoates and Their Cyclization to 4-Hydroxycoumarins via the N -Hydroxybenzotriazole Methodology. *Synthesis (Stuttg).* **2004**, *2004* (11), 1775–1782. https://doi.org/10.1055/s-2004-829132.

(3) Kraemer, J. F.; Lira, E. P. The Rearrangement of 4-hydroxyeoumarin Carbamates. *J. Heterocycl. Chem.* **1972**, *9* (3), 495–499. https://doi.org/10.1002/jhet.5570090306.

(4) Malta, O. L. Ligand—Rare-Earth Ion Energy Transfer in Coordination Compounds. A Theoretical Approach. *J. Lumin.* **1997**, *71* (3), 229–236. https://doi.org/10.1016/S0022-2313(96)00126-3.

(5) Malta, O. L.; Gonçalves e Silva, F. R. A Theoretical Approach to Intramolecular Energy Transfer and Emission Quantum Yields in Coordination Compounds of Rare Earth Ions. *Spectrochim. Acta Part A Mol. Biomol. Spectrosc.* **1998**, *54* (11), 1593–1599. https://doi.org/10.1016/S1386-1425(98)00086-9.

(6) Longo, R.; Gonçalves e Silva, F. R.; Malta, O. L. A Theoretical Study of the Energy-Transfer Process in $[Eu\subset bpy.Bpy.Bpy]^{3+}$ Cryptates: A Ligand-to-Metal Charge-Transfer State? *Chem. Phys. Lett.* **2000**, *328* (1–2), 67–74. https://doi.org/10.1016/S0009-2614(00)00898-8.

(7) Malta, O. L. Mechanisms of Non-Radiative Energy Transfer Involving Lanthanide Ions Revisited. *J. Non. Cryst. Solids* **2008**, *354* (42–44), 4770–4776. https://doi.org/10.1016/j.jnoncrysol.2008.04.023.

(8) Carneiro Neto, A. N.; Teotonio, E. E. S.; de Sá, G. F.; Brito, H. F.; Legendziewicz, J.; Carlos, L. D.; Felinto, M. C. F. C.; Gawryszewska, P.; Moura Jr., R. T.; Longo, R. L.; Faustino, W. M.; Malta, O. L. Modeling Intramolecular Energy Transfer in Lanthanide Chelates: A Critical Review and Recent Advances. In *Handbook on the Physics and Chemistry of Rare Earths, volume 56*; Bünzli, J.-C. G., Pecharsky, V. K., Eds.; Elsevier, 2019; pp 55–162. https://doi.org/10.1016/bs.hpcre.2019.08.001.

(9) Malta, O. L. Theoretical Crystal-Field Parameters for the $YOCl:Eu^{3+}$ System. A Simple Overlap Model. *Chem. Phys. Lett.* **1982**, *88* (3), 353–356. https://doi.org/10.1016/0009-2614(82)87103-0.

(10) Malta, O. L. A Simple Overlap Model in Lanthanide Crystal-Field Theory. *Chem. Phys. Lett.* **1982**, *87* (1), 27–29. https://doi.org/10.1016/0009-2614(82)83546-X.

(11) Moura Jr., R. T.; Carneiro Neto, A. N.; Aguiar, E. C.; Santos-Jr., C. V.; de Lima, E. M.; Faustino, W. M.; Teotonio, E. E. S.; Brito, H. F.; Felinto, M. C. F. C.; Ferreira, R. A. S.; Carlos, L. D.; Longo, R. L.; Malta, O. L. (INVITED) JOYSpectra: A Web Platform for Luminescence of Lanthanides. *Opt. Mater. X* **2021**, *11*, 100080. https://doi.org/10.1016/j.omx.2021.100080.

(12) Carnall, W. T.; Crosswhite, H.; Crosswhite, H. M. *Energy Level Structure and Transition Probabilities in the Spectra of the Trivalent Lanthanides in LaF_3*; Argonne, IL, United States, 1978. https://doi.org/10.2172/6417825.

(13) Carneiro Neto, A. N.; Moura Jr., R. T. Overlap Integrals and Excitation Energies Calculations in Trivalent Lanthanides 4f Orbitals in Pairs Ln-L (L = Ln, N, O, F, P, S, Cl, Se, Br, and I). *Chem. Phys. Lett.* **2020**, *757*, 137884. https://doi.org/10.1016/j.cplett.2020.137884.

(14) e Silva, F. R. G.; Malta, O. L. Calculation of the Ligand–Lanthanide Ion Energy Transfer Rate in Coordination Compounds: Contributions of Exchange Interactions. *J. Alloys Compd.* **1997**, *250* (1–2), 427–430. https://doi.org/10.1016/S0925-8388(96)02563-7.

(15) Ofelt, G. S. Structure of the f^6 Configuration with Application to Rare-Earth Ions. *J. Chem. Phys.* **1963**,

38 (9), 2171–2180. https://doi.org/10.1063/1.1733947.

(16) Kasprzycka, E.; Carneiro Neto, A. N.; Trush, V. A.; Jerzykiewicz, L.; Amirkhanov, V. M.; Malta, O. L.; Legendziewicz, J.; Gawryszewska, P. How Minor Structural Changes Generate Major Consequences in Photophysical Properties of RE Coordination Compounds; Resonance Effect, LMCT State. *J. Rare Earths* **2020**, *38* (5), 552–563. https://doi.org/10.1016/j.jre.2020.02.001.

(17) Riseberg, L. A.; Moos, H. W. Multiphonon Orbit-Lattice Relaxation of Excited States of Rare-Earth Ions in Crystals. *Phys. Rev.* **1968**, *174* (2), 429–438. https://doi.org/10.1103/PhysRev.174.429.

(18) Riseberg, L. A.; Weber, M. J. Relaxation Phenomena in Rare-Earth Luminescence. In *Progress in Optics*; 1977; Vol. 14, pp 89–159. https://doi.org/10.1016/S0079-6638(08)70251-8.

(19) Miyakawa, T.; Dexter, D. L. Phonon Sidebands, Multiphonon Relaxation of Excited States, and Phonon-Assisted Energy Transfer between Ions in Solids. *Phys. Rev. B* **1970**, *1* (7), 2961–2969. https://doi.org/10.1103/PhysRevB.1.2961.

(20) Yamada, N.; Shionoya, S.; Kushida, T. Phonon-Assisted Energy Transfer between Trivalent Rare Earth Ions. *J. Phys. Soc. Japan* **1972**, *32* (6), 1577–1586. https://doi.org/10.1143/JPSJ.32.1577.

(21) Fonger, W. H.; Struck, C. W. Unified Model of Energy Transfer for Arbitrary Franck-Condon Offset and Temperature. *J. Lumin.* **1978**, *17* (3), 241–261. https://doi.org/10.1016/0022-2313(78)90059-5.

(22) Auzel, F.; De Sá, G. F.; de Azevedo, W. M. An Example of Concentration Sensitive Electron-Phonon Coupling in $\{(C_4H_9)_4N\}_3$ $Eu_xY_{1-x}(NCS)_6$ and a New Hypothesis for Self-Quenching. *J. Lumin.* **1980**, *21* (2), 187–192. https://doi.org/10.1016/0022-2313(80)90020-4.

(23) Carneiro Neto, A. N.; Nasalska, J.; Gawryszewska, P.; Trush, V. A.; Sokolnicki, J.; Malta, O. L.; Legendziewicz, J. Intramolecular Energy Transfer and Its Influence on the Overall Quantum Yields of Eu^{3+} and Tb^{3+} Chelates with Dimethyl(Phenylsulfonyl)Amidophosphate Ligands. *Spectrochim. Acta Part A Mol. Biomol. Spectrosc.* **2025**, *324*, 124875. https://doi.org/10.1016/j.saa.2024.124875.

(24) Butcher, J. C. Numerical Methods for Ordinary Differential Equations in the 20th Century. *J. Comput. Appl. Math.* **2000**, *125* (1–2), 1–29. https://doi.org/10.1016/S0377-0427(00)00455-6.

(25) Hairer, E.; Wanner, G. Radau Methods. In *Encyclopedia of Applied and Computational Mathematics*; Engquist, B., Ed.; Springer Berlin Heidelberg: Berlin, Heidelberg, 2015; pp 1213–1216. https://doi.org/10.1007/978-3-540-70529-1_139.

(26) De, A.; Hernández-Rodríguez, M. A.; Carneiro Neto, A. N.; Dwij, V.; Sathe, V.; Carlos, L. D.; Ranjan, R. Resonance/off-Resonance Excitations: Implications on the Thermal Evolution of Eu^{3+} Photoluminescence. *J. Mater. Chem. C* **2023**, *11* (18), 6095–6106. https://doi.org/10.1039/D2TC03464F.

(27) Moura, R. T.; Quintano, M.; Santos-Jr, C. V.; Albuquerque, V. A. C. A.; Aguiar, E. C.; Kraka, E.; Carneiro Neto, A. N. Featuring a New Computational Protocol for the Estimation of Intensity and Overall Quantum Yield in Lanthanide Chelates with Applications to Eu(III) Mercapto-Triazole Schiff Base Ligands. *Opt. Mater. X* **2022**, *16*, 100216. https://doi.org/10.1016/j.omx.2022.100216.

(28) Carneiro Neto, A. N.; Moura, R. T.; Carlos, L. D.; Malta, O. L.; Sanadar, M.; Melchior, A.; Kraka, E.; Ruggieri, S.; Bettinelli, M.; Piccinelli, F. Dynamics of the Energy Transfer Process in Eu(III) Complexes Containing Polydentate Ligands Based on Pyridine, Quinoline, and Isoquinoline as Chromophoric Antennae. *Inorg. Chem.* **2022**, *61* (41), 16333–16346. https://doi.org/10.1021/acs.inorgchem.2c02330.

(29) Salerno, E. V.; Carneiro Neto, A. N.; Eliseeva, S. V.; Hernández-Rodríguez, M. A.; Lutter, J. C.; Lathion,

T.; Kampf, J. W.; Petoud, S.; Carlos, L. D.; Pecoraro, V. L. Tunable Optical Molecular Thermometers Based on Metallacrowns. *J. Am. Chem. Soc.* **2022**, *144* (40), 18259–18271. https://doi.org/10.1021/jacs.2c04821.

(30) Moura, J. L.; Costa, I. F.; Santos, P. R. S.; Silva, I. F.; Moura, R. T.; Carneiro Neto, A. N.; Faustino, W. M.; Brito, H. F.; Sabino, J. R.; Teotonio, E. E. S. Enhancing the Luminescence of Eu(III) Complexes with the Ruthenocene Organometallic Unit as Ancillary Ligand. *Inorg. Chem.* **2022**, *61* (34), 13510–13524. https://doi.org/10.1021/acs.inorgchem.2c02115.

(31) Carneiro Neto, A. N.; Kasprzycka, E.; Souza, A. S.; Gawryszewska, P.; Suta, M.; Carlos, L. D.; Malta, O. L. On the Long Decay Time of the $^7F_5$ Level of Tb^{3+}. *J. Lumin.* **2022**, *248* (7), 118933. https://doi.org/10.1016/j.jlumin.2022.118933.

(32) Carneiro Neto, A. N.; Mamontova, E.; Botas, A. M. P.; Brites, C. D. S.; Ferreira, R. A. S.; Rouquette, J.; Guari, Y.; Larionova, J.; Long, J.; Carlos, L. D. Rationalizing the Thermal Response of Dual-Center Molecular Thermometers: The Example of an Eu/Tb Coordination Complex. *Adv. Opt. Mater.* **2022**, *10* (5), 2101870. https://doi.org/10.1002/adom.202101870.

(33) Blois, L.; Carneiro Neto, A. N.; Malta, O. L.; Brito, H. F. The Role of the Eu^{3+} $^7F_1$ Level in the Direct Sensitization of the $^5D_0$ Emitting Level through Intramolecular Energy Transfer. *J. Lumin.* **2022**, 118862. https://doi.org/10.1016/j.jlumin.2022.118862.